

NPS ARCHIVE
1968
SHOEMAKER, W.

NANOSECOND R-F PULSES FOR
WAVEGUIDE FAULT-FINDING

by

William Bruce Shoemaker, Jr.

UNITED STATES NAVAL POSTGRADUATE SCHOOL



THESIS

NANOSECOND R-F PULSES FOR
WAVEGUIDE FAULT-FINDING

by

William Bruce Shoemaker, Jr.

September 1968

~~This document is subject to special export con-
trols and its transmittal to foreign government
or foreign nationals may be made only with prior
approval of the U. S. Naval Postgraduate School.~~

NANOSECOND R-F PULSES FOR
WAVEGUIDE FAULT-FINDING

by

William Bruce Shoemaker, Jr.
Lieutenant, United States Navy
B.S., United States Naval Academy, 1961



Submitted in partial fulfillment of the
requirements for the degree of
MASTER OF SCIENCE IN ELECTRICAL ENGINEERING
from the
NAVAL POSTGRADUATE SCHOOL
September 1968

NPS Archive
1968
Shoemaker, W.

~~RRD~~ ~~S4783~~ c.1

ABSTRACT

A system has been developed for the location of waveguide discontinuities using nanosecond radio-frequency pulses with time-domain reflectometry techniques. The r-f pulse generation method used is discussed as well as the alternative methods investigated. Measurement-system design and procedures are outlined. Resolution on the order of 4 feet for reflections over 45-db return loss and accuracy of 2 per cent as compared to conventional methods are reported and various measurement examples are presented.

Significant advantages of this system appear in locating imperfections in waveguides and other bandpass transmission systems, as compared to conventional c-w-standing-wave or trial-and-error methods.

TABLE OF CONTENTS

<u>Chapter</u>	<u>Page</u>
I. Introduction	13
II. Pulse Generation Methods	21
A. Phase-Coherent Pulse Methods	21
B. Noncoherent Pulse Methods	22
III. Waveguide Testing System	33
A. Set-up Description	33
B. Calibration and Correction for Variations in System Response	35
C. Measurement Procedures	38
IV. Test Samples	44
A. Mismatches Due to Differences in Internal Waveguide Dimensions within the Allowable Tolerances	44
B. Reflections from Various Waveguide Components	50
C. Variation of Propagation Velocity and Attenuation with Frequency	53
D. Delay Distortion	56
E. Radar Waveguide System Tests	59
V. Conclusions	84
Bibliography	87
Appendix	88

LIST OF TABLES

Table	Page
1. Sliding load measurements	41
2. Summary of measurement results	48
3. Internal waveguide dimensions	48
4. SS waveguide measurement data	63
5. MK 13 waveguide measurement data	73
6. MK 25 waveguide measurement data	78

LIST OF ILLUSTRATIONS

Figure	Page
1. Propagation constant versus frequency for lossless RG-51 waveguide	16
2. Coaxial quarter-wave cavity	23
3. Phase-coherent TDR system	23
4. Phase-coherent pulse	24
5. Incident and reflected pulses	24
6. Thyatron pulse generator	26
7. Thyatron pulse across 1-K resistor	26
8. Pulse generation by helix modulation	28
9. Detected r-f pulse due to helix modulation . . .	28
10. Modulator output pulse	29
11. Detected r-f pulse	29
12. Noncoherent pulse generator	31
13. TDR set-up	34
14. Detector response curves	36
15. Moveable-load reflection coefficient versus frequency	42
16. Sliding load reflections	42
17. Coupling return loss measurement	44
18. Types of sliding termination	45
19. Case I: termination number 1	47
20. Case II: termination number 2	47
21. Case III: termination number 1 with reflecting foil	47
22. Load-return legend	47

Figure	Page
23. Bench set-up	50
24. Reflection without test component	51
25. 90 degree twist	51
26. Matched termination	51
27. 90 degree E bend	52
28. 90 degree E bend	52
29. Flat flange to choke flange connection	52
30. Set-up for RG-52	53
31. Multiple reflections from shorted waveguide section	54
32. Variation of attenuation and propagation velocity with frequency	54
33. Delay distortion	58
34. SS radar waveguide installation	60
35. SS radar waveguide reflections	61
36. SS radar waveguide reflections, expanded time scale	61
37. SS waveguide reflections	63
38. Legend for SS waveguide reflections	63
39. SS radar waveguide reflections at frequencies 8.5-9.1 GHz.	64
40. SS radar waveguide reflections at 8.8 GHz	65
41. Swept-frequency measurement of reflection coefficient	67
42. Multiple exposure of SS radar waveguide reflections from 8.5-9.1 GHz in 50 MHz steps	69

Figure	Page
43. Voltage reflection coefficient versus frequency for SS radar waveguide	70
44. L-band test set-up	71
45. MK 13 radar waveguide installation	72
46. MK 13 radar waveguide reflections	73
47. Legend for MK 13 radar waveguide reflections . .	73
48. MK 13 radar waveguide reflections at frequencies 8.5-9.1 GHz	74
49. MK 13 radar waveguide reflections at 8.80 MHz. .	75
50. Multiple exposure of MK radar waveguide reflections at 8.5-9.1 GHz in 50 MHz steps . . .	75
51. Voltage-reflections coefficient versus frequency for MK 13 radar waveguide.	76
52. MK 25 radar waveguide installation	77
53. MK 25 radar waveguide reflections	78
54. Legend for MK 25 radar waveguide reflections . .	78
55. MK 25 radar waveguide reflections at frequencies 8.8-9.35 GHz	79
56. MK 25 radar waveguide reflections at 9.10 GHz. .	80
57. Multiple exposure of MK 25 radar waveguide reflections at frequencies from 8.8-9.35 GHz in 50 MHz steps	80
58. Voltage reflection coefficient versus frequency for MK 25 radar waveguide	81
59. L-band radar waveguide reflections	82

ACKNOWLEDGMENTS

This project was suggested by Professor David B. Moisington who acted as advisor. Sincere appreciation is expressed for his patience and continued guidance. In addition much gratitude is extended to Professor George L. Sackman for technical assistance and advice.

Further acknowledgment is in order to my wife for suggestions in composition, typing, and general assistance beyond the call of duty. Due special thanks is Mrs. Donald E. Christy whose nimble fingers did the bulk of first draft typing and retyping.

CHAPTER I

INTRODUCTION

Pulse techniques have long been utilized for the investigation of transmission line discontinuities. These techniques have been used since 1940 in cases where the time scale has permitted measurements with microsecond pulses and megahertz bandwidths. By "pulse techniques" is meant the sending of a pulse of energy into a transmission line and observing on an oscilloscope the echos returned from discontinuities. The most important advantage of such a technique is the determination of the distance to the point of the discontinuity by means of measuring the elapsed pulse travel time. If the time scale were changed to permit measurements with r-f pulses of nanosecond duration and hundreds of megahertz bandwidths, such a technique would have direct applicability to the testing of all types of waveguide installations. Such a procedure would give an indication not only of the faulty component or section, but also of the seriousness of the defect in terms of percent power reflected. As applied to radar waveguides, this technique would be, in effect, a radar within a radar.

The first practical application of pulse techniques (or what has come to be known as time-domain reflectometry) occurred in 1940 when the "coaxial pulse-echo set" was used to control the manufacture of coaxial cables.¹ This set used a d-c pulse that was variable in width over a range

of 0.25-1.5 microseconds and was able to measure to about plus or minus 50 feet. This set was improved upon and its use extended to include field testing of cables to insure proper installation, to locate discontinuities, and to set limits on defects. The second practical device was the "Lookator", which was built by Bell Laboratories for the Signal Corps during World War II.² This device applied the same principles to testing spiral-four-conductor field cable and open-wire lines.

A more recent advance in TDR techniques has been the development of a laboratory time-domain reflectometer employing a step-function with a 150-ps risetime and a sampling oscilloscope with a 2.3 GHz bandwidth.² This method allows resolution to within a few inches. Currently available pulse generators and oscilloscopes having 30-ps risetimes and 12 GHz bandwidths permit higher resolution. This method requires that the transmission system to be tested have a bandwidth commensurate with the step or pulse spectrum (extending to d-c). It is this requirement that prevents such TDR techniques from being used successfully on waveguide systems. Waveguides are by nature "bandpass" transmission systems. The low-frequency limit is set by waveguide cutoff and delay distortion, and the high-frequency limit by higher-order mode considerations. A d-c step or pulse has a spectrum with a large d-c component and with most other components in the vicinity of d-c. A pulse of carrier on the other hand, would have all frequency components within the waveguide passband, provided the pulse width was wide enough.

A step-function could conceivably be used for waveguide fault-finding if sufficient energy were coupled in the waveguide passband. However, over a wide band the frequency response of waveguides is far from ideal. Both the amplitude and the phase response deviate widely with frequency. Low-frequency components below cutoff are not propagated while components somewhat above cutoff have lower group velocities than at midband. In the other direction, high-frequency components give rise to higher order mode reflections, the group velocities of which depend on the mode. In addition the amplitude response is definitely not constant since attenuation varies with mode and frequency. These effects cause severe distortion of the waveform reflected from waveguide discontinuities when a d-c step or pulse is employed for testing. The use of pulse TDR techniques with waveguide systems therefore requires a generation and detection method utilizing waveforms with frequency components which fall in a restricted usable band within the passband of the waveguide. The restricted usable band is determined by a trade-off between the resolution required and the distortion which can be tolerated.

Figure 1 shows the propagation constant versus angular frequency for lossless RG-51 waveguide. Superimposed on this is a plot of the frequency spectrum of a 150-ps-rise-time step (A), a 0.5-ns d-c pulse (B), a 2.5-ns pulse of 9-GHz carrier (C), and a 10-ns pulse of 9-GHz carrier (D). The step and d-c pulse spectrums shown have bandwidths

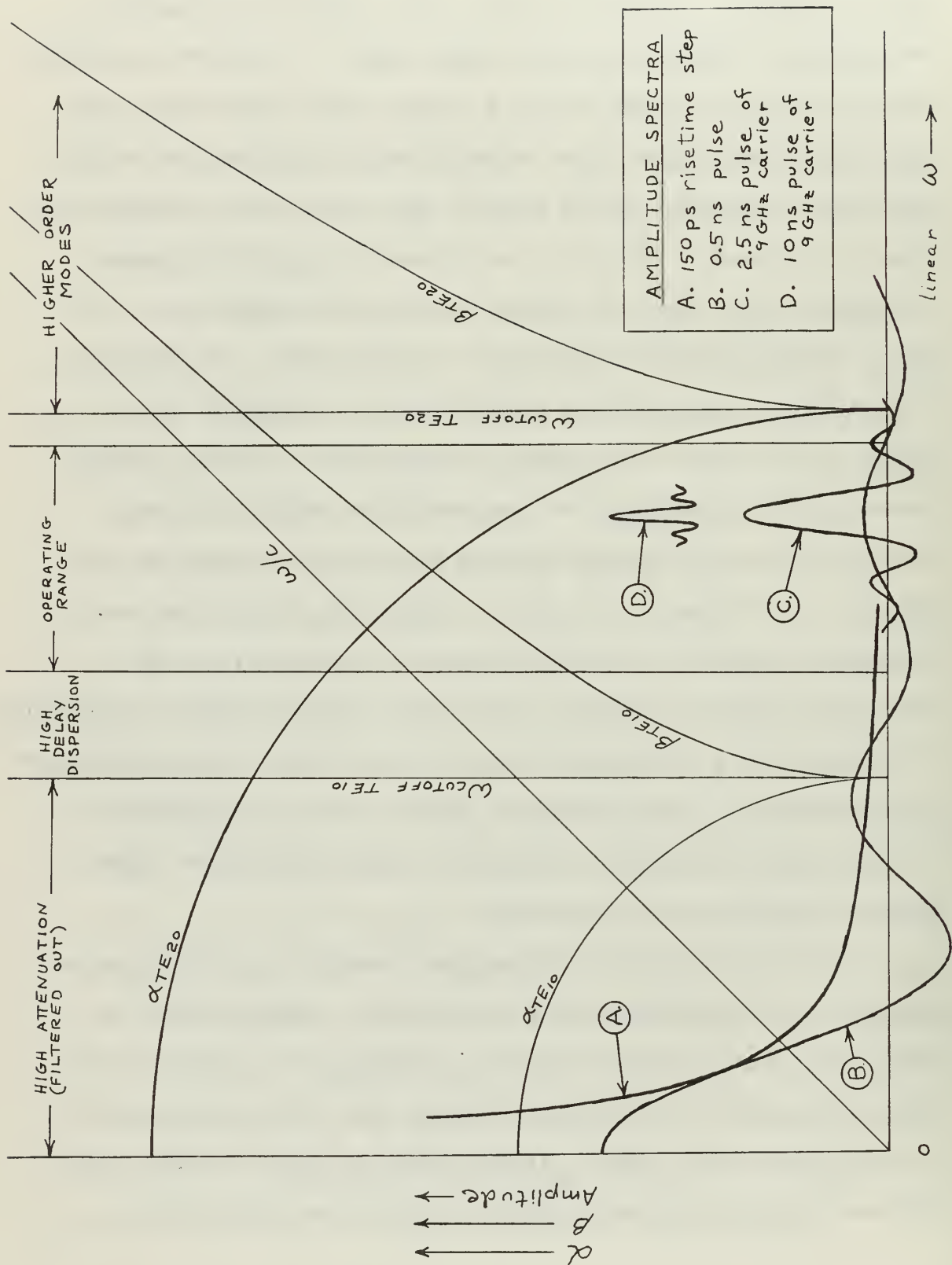


Figure 1. Propagation constant versus frequency for lossless RG-51 waveguide.

comparable to those of currently used TDR system waveforms. In both cases most of the signal is filtered out because it is outside of the waveguide passband. Case C is the spectrum of a 2.5-ns pulse of 9-GHz carrier having the maximum bandwidth (400 MHz) permitted by delay distortion when used in a 100-foot section of waveguide. Case D is the spectrum of a pulse comparable in width to the pulse used in this experimental system for TDR waveguide investigation.

The problems inherent in step-waveform TDR methods are therefore solved by narrowing and translating in frequency the spectrum of the TDR waveform to be used for testing. The narrower the band the closer the waveguide frequency response approaches that of constant amplitude and linear phase at the price of resolution.

In addition to time-domain methods, frequency-domain reflectometry (FDR) techniques have also been employed for the location of waveguide discontinuities.³ FDR locates defects by sweeping the input to a system over a band of frequencies within the system's passband and analyzing the reflected returns. Location of a fault is derived from measurement of the frequency difference between adjacent standing-wave ratio (SWR) maxima or minima that occur during the sweep. This method is usable when the number of waveguide discontinuities is low and the SWR is relatively high. For practical waveguide installation, however, the large number of discontinuities causes a very complex SWR-versus-frequency

relationship which makes interpretation of the display extremely difficult and fault location very complicated.

For the above reasons a band-limited, pulsed TDR system must be designed specifically for waveguides in order to be useful for the investigation of discontinuity location and amplitude.

The object of this thesis work is to extend time-domain reflectometry techniques to waveguide or band-limited coaxial systems using the equipment on hand and to design a simple system, along with associated procedures, for locating and measuring discontinuities. It is hoped that this may serve as a basis for a future test-set to be used in shipboard or shore-based waveguide trouble-shooting or installation. It is envisioned that such a package could ultimately be achieved in solid state by using, for example, one of the bulk negative-resistance devices driven by a diode pulser.

The reason for investigation of time-domain reflectometry techniques stems from the difficulty of isolating a fault in a waveguide. Current waveguide standards are based on standing-wave ratio (SWR) measurements taken of the entire system by either directional-coupler or slotted-line techniques. The system SWR thus obtained is a result of the vector addition of the reflections due to all of the discontinuities. The resulting SWR is therefore determined by the amplitudes and relative phase relationships due to all discontinuities. If the measured SWR is above the acceptable limit for a given system, time-domain reflectometry techniques

could be used to discover directly the source of the problem. On the other hand, there is the possibility that the system SWR measures within standards and yet the waveguide contains discontinuities which will break down under high-power application. This is because the discontinuities have phase relationships such that their effects may cancel at the point of SWR measurement. A system could in fact measure within SWR standards and still be susceptible to breakdown at high-power levels due to multiple high-attenuation discontinuities. Pulse methods could be used to locate such discontinuities if the discontinuities were separated by more than one half the distance the pulse occupies (the pulse resolution distance) in its travel down the waveguide. Only those discontinuities which are thus separated will have noninteracting reflections. The way the waveguide "looks" to a time-domain reflectometry (TDR) system is not the way it "looks" to a radar pulse under normal operation, since the TDR pulse has a much wider frequency bandwidth and is likely to "see" more faults than a narrower-bandwidth radar pulse. This is because each discontinuity or group of discontinuities within the resolution distance is frequency dependent. Therefore the wider the bandwidth of the pulse used to "illuminate" the waveguide the more discontinuities which will show up. From the time-domain point of view this simply means that a radar pulse duration is too long to resolve waveguide discontinuities.

To obtain the highest degree of resolution requires the generation of as narrow a pulse as possible without distortion.

To obtain 5-foot resolution the pulse should have a length of no more than 10 feet in the waveguide. At a carrier frequency of 9 gigahertz such a pulse contains less than 100 cycles of radio-frequency energy and is on the order of 10 nanoseconds in duration. The bandwidth required for such a pulse is about 100 megahertz. The system for generation, amplification, reception and display of such a pulse must necessarily be broadband.

Thus, in summary, the primary advantage of the time-domain reflectometry system is the location (to within the pulse resolution distance) of faults. Another benefit is the possibility of locating faults which would not otherwise show up from SWR measurements, and yet would be sources of power loss or waveguide breakdown during actual operation. This work extends the advantages of TDR to waveguide systems.

CHAPTER II

PULSE GENERATION METHODS

A. Phase-Coherent Pulse Methods

The first idea considered for implementing a waveguide time-domain reflectometer system was the generation of phase-coherent microwave pulses which could be used to obtain both phase and amplitude information about the waveguide discontinuities. A method for the generation of this form of energy by weighting, delaying, combining and filtering a fast d-c step is described by G. F. Ross.³ Briefly, the method consists of a fast step generator, the output of which is fed into a parallel-series network of various lengths to give out a fixed number of radio-frequency cycles. A wideband sampling oscilloscope is required for display.

A crude model was constructed using RG-58 coaxial cable, and was driven by the step output of a Hewlett-Packard Time-Domain Reflectometer (1415A) plug-in unit for a HP-140A oscilloscope. Four cycles at about 1 gigahertz were obtained and viewed on a 1-gigahertz sampling oscilloscope. A disadvantage inherent in this pulse generation technique is the finite residue (30 db down) which exists following the pulse. This method was abandoned due to construction difficulties, the unavailability of a broader-bandwidth sampling oscilloscope, the fact that such techniques are limited at present to about L and S bands, and the presence of this residue following the main pulse.

The next approach to the generation of a phase-coherent pulse was an attempt to shock-excite a low-Q cavity in order to obtain a fast-decaying r-f pulse. Toward this end a quarter-wave coaxial cavity was constructed as shown in Figure 2 and used in the setup of Figure 3. Input and output coupling were as shown in the figure. The Q of the cavity was found to be about 25. The pulse generated by this cavity is shown in Figure 4.

The pulse is approximately 5 nanoseconds wide, with a carrier frequency of 900 megahertz. Reflections received from the end of a 7.5-foot length of RG-58 are shown in Figure 5. Case I is for an open line and Case II is for a shorted line. Note the 180-degree phase reversal in the reflection due to the short.

The pulse generated by this method was then amplified by an L-band, traveling-wave tube to a peak power of approximately eight milliwatts. The method looked quite promising, but was not pursued for two reasons. First, an increase in frequency into the L-band operating range of radars using RG-69 waveguide would exceed the bandwidth of the oscilloscope; and second, an additional L-band, TWT amplifier was not available to increase the pulse power to a usable level.

B. Noncoherent Pulse Methods

In order to overcome the equipment problem at L-band and higher frequencies, it was decided to go to a system using a noncoherent pulse. The bandwidth problem was solved by detecting the pulse r-f envelope, the video bandwidth

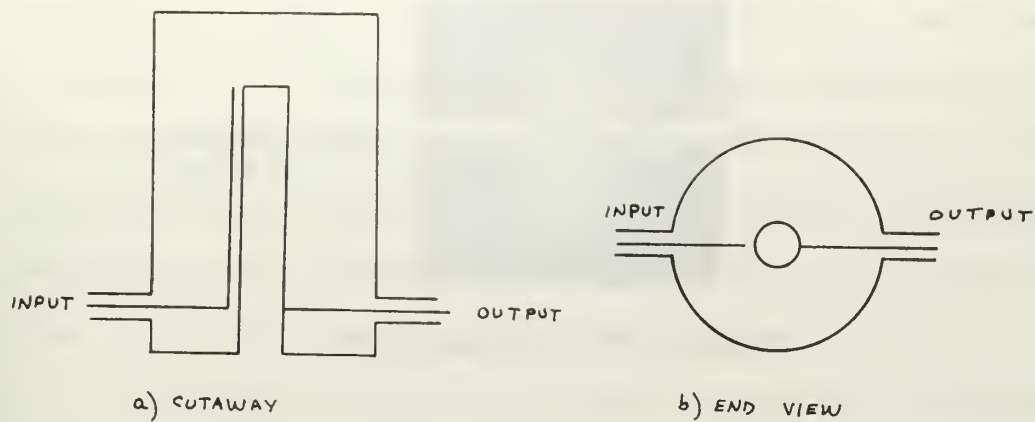


Figure 2. Coaxial quarter-wave cavity.

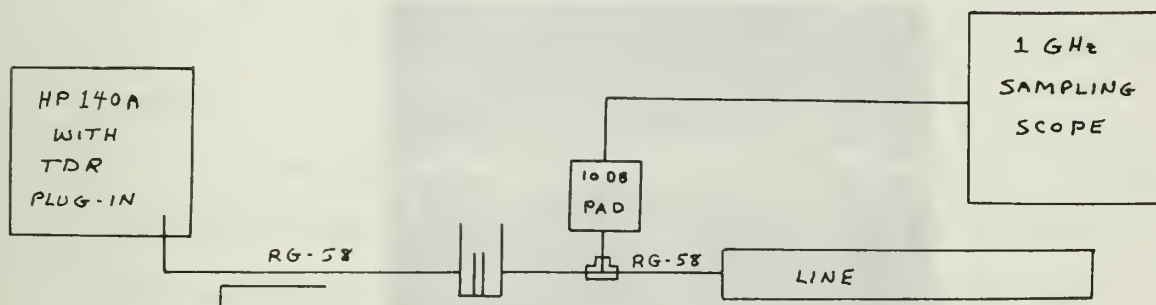
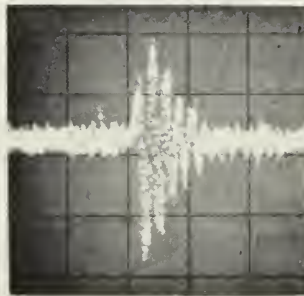
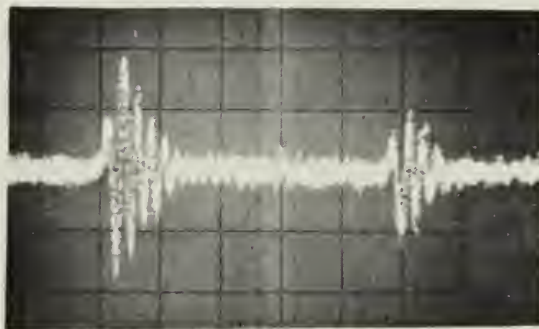


Figure 3. Phase-coherent TDR system.



Scale: 5 ns/cm
2 mv/cm

Figure 4. Phase-coherent pulse.



Case I: open line

Scale: 5ns/cm
2mv/cm



Case II: shorted line

Figure 5. Incident and reflected pulses.

being well within the sampling oscilloscope's 1-GHz bandwidth. The other difficulties were largely solved by going to X-band, where considerable laboratory equipment was available. It should be noted that any of the noncoherent methods discussed could be made coherent by using a stable oscillator and synchronized pulser. However this would complicate the system and would also be self-defeating since the r-f envelope is to be detected anyway.

In 1955 A. C. Beck performed waveguide tests using time-domain reflectometry techniques.⁴ For this he used a 5 to 6 nanosecond-long pulse at a frequency of 9 GHz. This pulse was obtained by driving the helix of a traveling-wave-tube amplifier through the operating region by application of a 500-volt, fast-rise, d-c pulse. Two r-f pulses were actually obtained, one during each traversal of the helix through its operating region. The second pulse was eliminated by gating the grid off during the fall of the helix pulse.

In an attempt to duplicate this procedure, a miniature thyatron was used to discharge a capacitor through a 1,000-ohm resistor, to obtain a fast-rising pulse of about 170-volt amplitude. The thyatron was triggered by a General Radio 1217-C pulse generator at a rate of about 12-KHz the maximum repetition frequency the circuit would allow. The thyatron circuit used is shown in Figure 6 and the pulse obtained across the 1,000-ohm resistor is shown in Figure 7.

Applying this pulse to the helix-modulation input of a Hewlett-Packard-494A-TWT amplifier, it was then possible to

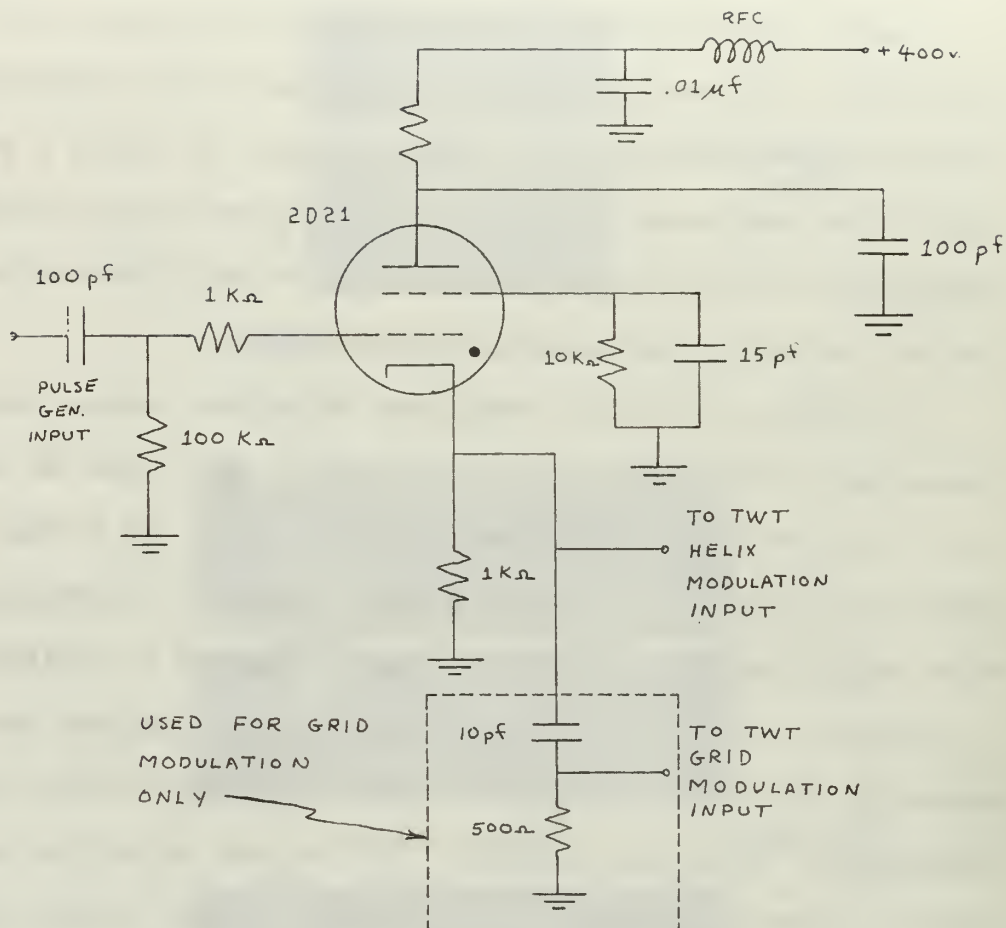
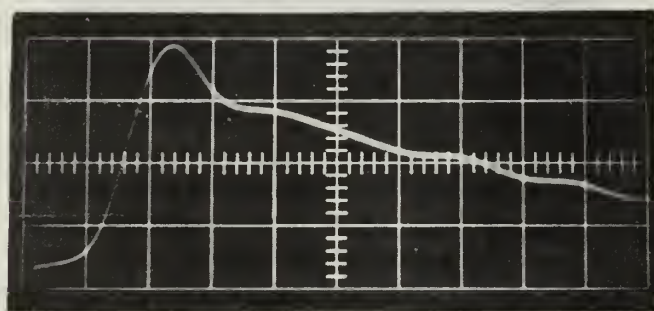


Figure 6. Thyatron pulse generator



Scale: 20 ns/cm
50 v/cm

Figure 7. Thyatron pulse across 1-K resistor.

drive the helix voltage to about 20 volts on either side of cutoff, and to obtain two r-f pulses at 9 GHz whose widths corresponded to the rise-time and fall-time of the helix voltage. The second pulse was gated off by application of a delayed pulse (obtained from a second pulse generator as shown in Fig. 8) to the grid of the TWT. The envelope of the r-f pulse thus generated had a 3-db width of just under 10 nanoseconds and is shown in Figure 9.

The difficulty with this method was in getting a "clean" r-f pulse, which is believed to be caused by operating too close to the helix cutoff. This was made necessary by the limited output available from the modulator. The system was very sensitive to the klystron output level, and in particular to the helix bias level. If one or the other of these were slightly misadjusted, either multiple r-f pulses were produced or excessive r-f leakage through the TWT amplifier developed.

During the course of the investigations, it was noted that the TWT was completely cut off with only minus 20 volts applied to the grid. Since the thyatron-pulse risetime is on the order of nanoseconds, it became apparent that if the falltime could be improved, then this pulse could be used to modulate the grid directly, without the helix modulation. For this purpose, the thyatron pulse was differentiated by applying it to the R-C combination that is also shown in Figure 6. The d-c pulse thus obtained has 55-volt-peak amplitude and is about 17 nanoseconds wide at the 3-db points, as viewed on the oscilloscope in Figure 10.

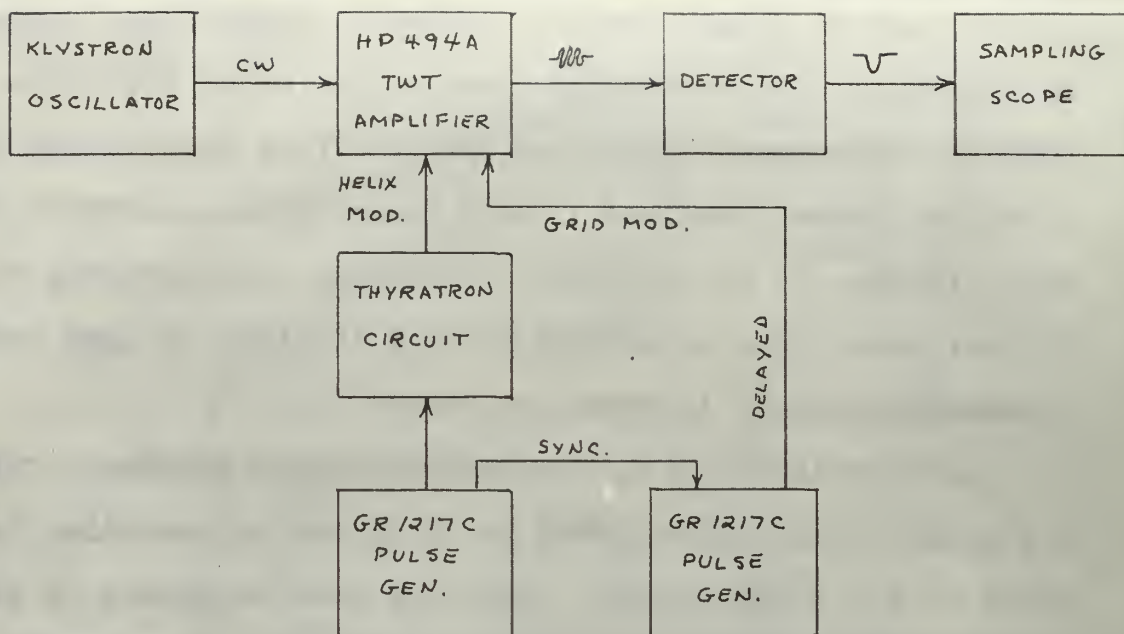
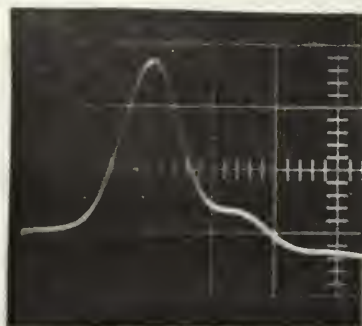


Figure 8. Pulse generation by helix modulation.



Scale: 10 ns/cm
20 mv/cm

Figure 9. Detected r-f pulse due to helix modulation.



Scale: 20 ns/cm
20 v/cm

Figure 10. Modulator output pulse



Scale: 10 ns/cm
20 mv/cm

Figure 11. Detected r-f pulse.

Since the risetime of the oscilloscope is about 15 ns, the pulse is in reality narrower than that displayed in Figure 10. This pulse was in turn applied to the TWT-amplifier, grid-modulation circuit with the grid bias set full negative (-50 volts). The r-f pulse thus generated has a half-power bandwidth just under 10 nanoseconds as shown in Figure 11. In this case however, it was possible to obtain 50 percent more power than with the helix modulation method, and without the critical tuning required to prevent multiple pulses or excessive leakage.

Two additional noncoherent pulse-generation techniques were considered which are worth mentioning briefly. The first is a method used by H. T. Closson of S-F-D Laboratories which involves the use of a waveguide hybrid junction.⁵ A fast r-f pulse is generated by means of the switch action of the hybrid junction. The two symmetric arms of the hybrid junction are terminated with tunable waveguide-detector mounts containing standard IN23 video crystals. If a c-w signal is sent into one antisymmetric arm and the two symmetric arms are matched with the diodes back-biased, power will then be equally divided between them and no power will propagate out of the other antisymmetric arm. However, if one of the diodes is forward biased momentarily, the bridge will be unbalanced and a pulse of r-f power, the width of which is determined by the width of the unbalancing pulse, will leave the other antisymmetric arm. By means of this method Closson was able to generate r-f pulse widths on the

order of 2 ns with an insertion loss greater than 20 db between the antisymmetric arms when the bridge was balanced. Except for the pulser, this is an excellent method simply because it can be achieved with readily available equipment.

The final noncoherent pulse-generation method considered was that of C. A. Burrus of Bell Laboratories in which he obtained a 3-nanosecond X-band pulse by means of a ferrite circulator and a point-contact crystal diode used as a resonant-waveguide switch.⁶ This method at X-band was a step toward the development of a similar pulse in the millimeter region. A diagram of this method is shown in Figure 12.

A short, forward-bias pulse is applied to the waveguide switch to momentarily short the waveguide and reflect a pulse of r-f energy back through the circulator and out of port 3. The advantages of this method over the previous one include very low residual energy and a more stable source due to the excellent impedance match provided at all times.

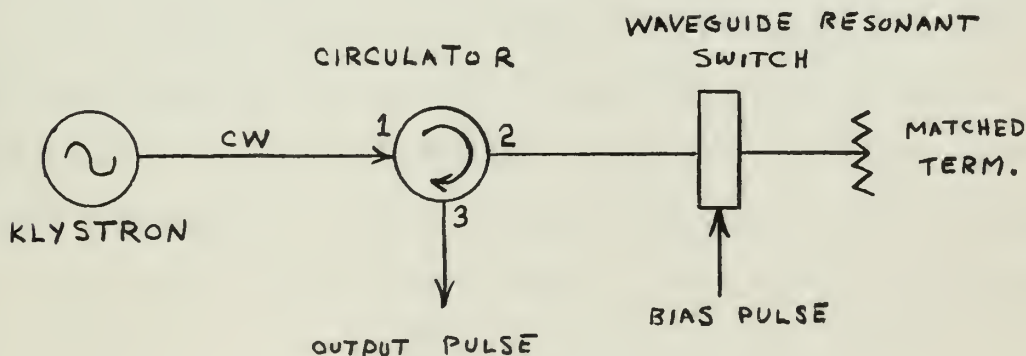


Figure 12. Noncoherent pulse generator.

In the final analysis, the TWT grid-modulation method was selected because of its better stability over the helix-modulation method, and also because it could be accomplished with currently available equipment. It was felt that if waveguide measurement results using this pulse showed promise, later research could be directed toward developing a pulse-generation method more suitable for assembly in a single test package.

CHAPTER III

WAVEGUIDE TESTING SYSTEM

A. Set-up Description

The radio-frequency pulse produced by grid modulation of a TWT, as described in Chapter II, has a peak power of 50 milliwatts. This pulse is further amplified by a second TWT to a peak power of about 2 watts. The system developed for the employment of this pulse in waveguide reflectometry is shown in Figure 13.

The pulse is fed into a ferrite circulator through port one, leaves port 2 and is sent via a waveguide shorting switch to the waveguide being tested. The circulator provides about 40 db of isolation for the return-echo detector. A sample of the incident pulse is obtained with a 20-db directional coupler. This is detected and displayed on the lower trace of the sampling oscilloscope, as a time reference. The echos from waveguide discontinuities return to the circulator through port 2, and travel out port 3 to be detected and displayed on the upper trace of the oscilloscope.

The waveguide shorting switch is placed at a position such that the electrical path length from port 1 of the circulator to detector 2 equals the path length from port 1 of the circulator to the shorting switch and back to detector 1. This allows the shorting switch to be used as the measuring reference, corresponding to the zero time position of the incident pulse sample on the oscilloscope.

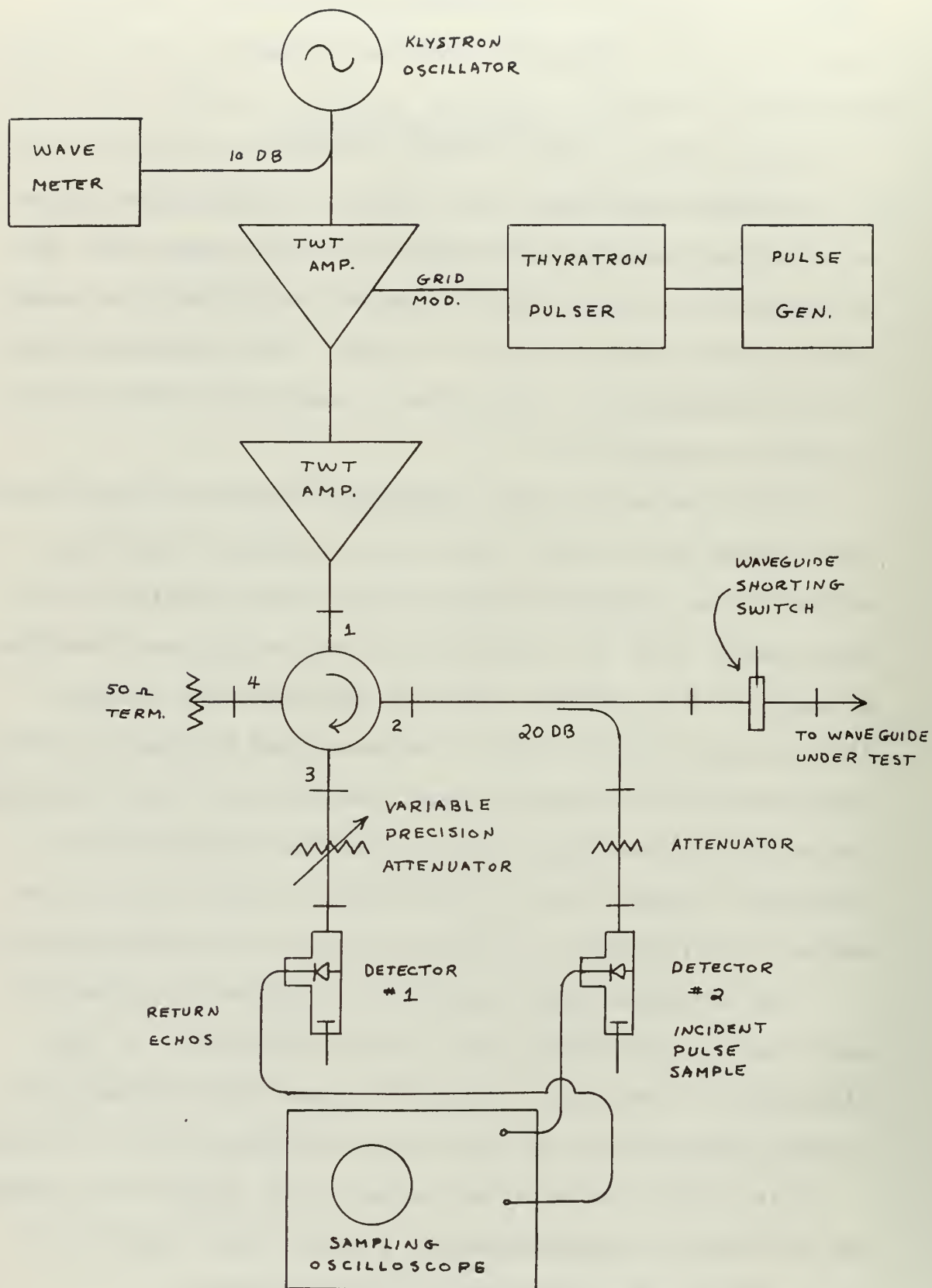


Figure 13. TDR Set-up.

B. Calibration and Correction for Variations in System Response.

As a first step in determining the system effectiveness, a set of response curves were taken of the detector to be used for the return echos. This was an HP-X485B waveguide detector mount with an IN23NE crystal diode with output terminated by a 40-ohm coaxial resistor. The sampling oscilloscope was used as the indicator. Response curves were run for frequencies 8.2, 8.6, 9.0, 9.5, and 10.0 gigahertz. These are shown in Figure 14. It was noted that the detector required tuning, not only with a change in frequency, but also with changes in power level for a given frequency. The tuning position was nearly constant for the mid-power level ranges, but varied substantially at the high and low levels.

The following technique was developed as a means of obtaining measurement accuracies which were independent of not only the detector response variations, but also most other system loss variations as well. After adjusting the power levels for proper pulse generation, the waveguide shorting switch is closed. The pulse reflected by the switch is used as the reference power level. The precision attenuator is adjusted to a value such that the displayed pulse level on the oscilloscope is lower than the echo to be measured. Detector number 1 is tuned to give maximum response to this power level. This level is noted and the waveguide switch is opened, permitting the display of the return echoes. The precision attenuator is again adjusted so that the echo-pulse level to be measured is matched with

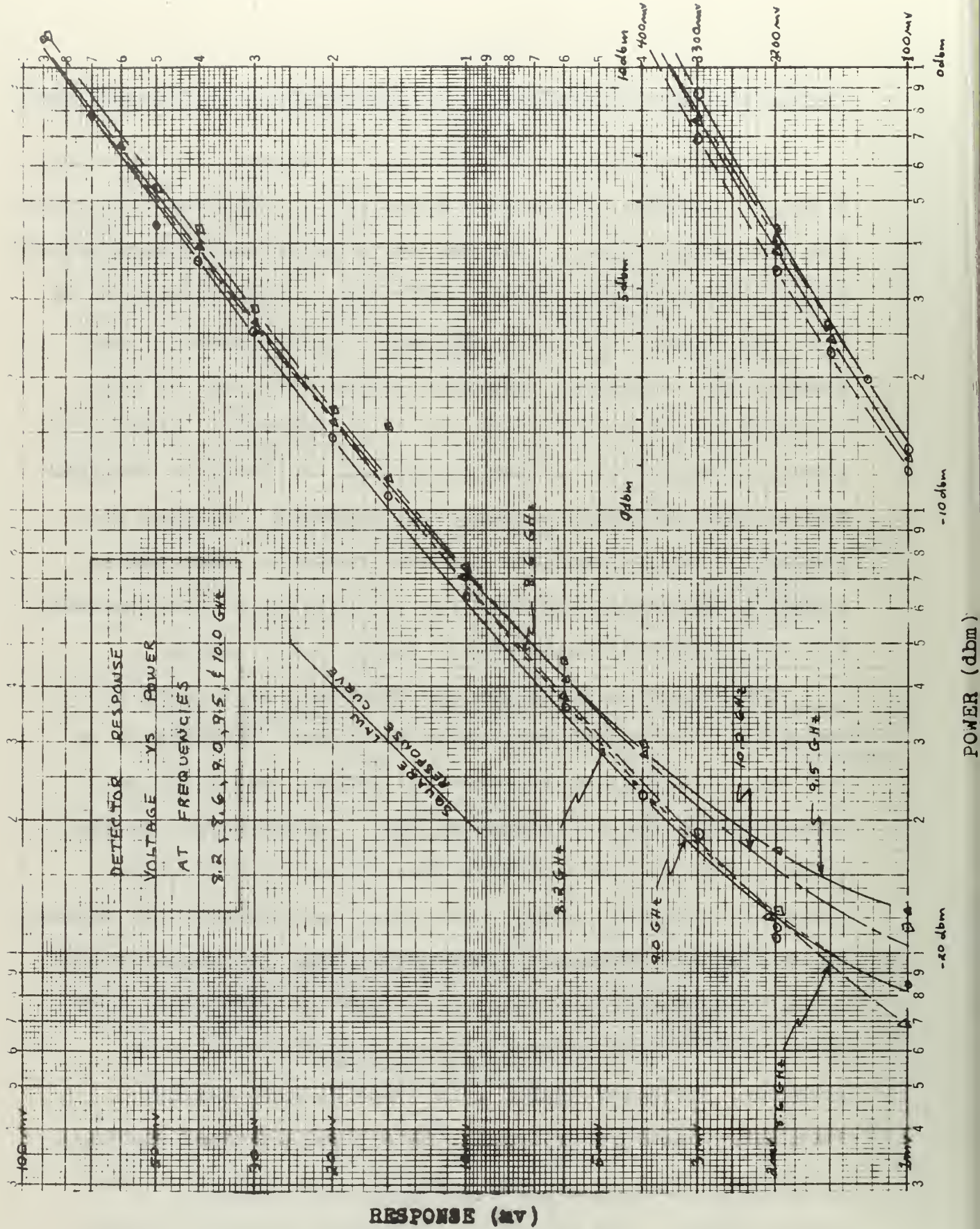


Figure 14. Detector Response Curves.

the previously noted level. The difference in the precision attenuator readings is the ratio of the echo level to that of the reference. This difference in db is defined as the apparent return loss due to a given discontinuity (L_{Rapp}). It is called the apparent return loss because it must be adjusted for waveguide losses to become the return loss (L_R) at the point of discontinuity.

Since this measurement is made using the same power level at the detector, its accuracy depends on only two factors: (1) how well the shorted waveguide switch approximates a perfect short, and (2) the accuracy of the precision attenuator. As given by the manufacturer's specifications, the waveguide shorting switch deviates from a perfect short by less than 0.13 db, and the accuracy of the precision attenuator is within $\pm 2\%$ of the scale reading in db.

The expression for the return loss of any discontinuity is given by:

$$L_{R_x} = L_{\text{Rapp}_x} - 2a_{l_x} - 2 \sum_{k=1}^{x-1} L_{T_k} \quad (1)$$

where:

x = discontinuity number, starting at the near end of the waveguide.

L_{R_x} (return loss of discontinuity x) = $10 \log \frac{\text{incident power}}{\text{reflected power}}$ referred to discontinuity x at the location of the discontinuity.

L_{Rapp_x} (apparent return loss of discontinuity x) = $10 \log \frac{\text{incident power}}{\text{reflected power}}$ referred to discontinuity x as measured at the waveguide input.

$2a_{l_x}$ = two-way attenuation to the point of discontinuity.

L_{Tx} (transmission loss of discontinuity x) = $10 \log \frac{\text{power incident}}{\text{power transmitted}}$ referred to discontinuity x at the point of the discontinuity.

For waveguide systems with no major discontinuities, the last term in the expression for return loss may be omitted without significantly affecting the results. Even when troubleshooting a waveguide, the last term can be omitted for the practical reason that if a fault is too large to "see through", then it will have to be repaired in any case. If, however, it is necessary to "look through" a major fault, it is a simple matter to include the transmission loss of this fault as the final term when measuring discontinuities beyond it.

C. Measurement Procedures

Before the return loss of each discontinuity could be calculated, it was necessary to find at the frequency of measurement the attenuation and group velocity for the particular waveguide to be measured. This was done by measuring the pulse power returned and the time elapsed from a copper shorting plate inserted at the most distant accessible flange in the waveguide installation. For example, in the radar waveguide system using RG-51, the frequency used was

8.80 GHz. The measured attenuation was 0.0386 db/ft corrected for the intervening transmission losses. The two-way group velocity at 8.8 GHz measured 0.380 round-trip feet per nanosecond. This value was lower than the theoretically calculated value by 0.014 feet per nanosecond.

A sizeable difference was discovered when comparing the measured attenuation for copper waveguide with the theoretical attenuation, which is 0.0221 db per foot for RG-51 at 8.8 GHz. This difference, it was found, was due to a layer of zinc chromate on the inner surfaces of the waveguides tested. The application of zinc chromate to the interior of copper waveguide is specified in the Electronics Installation and Maintenance Book: Installation Standards (NAVSHIPS 0967-000-0110, Change 5, May 1966, p. 5-14-4). Measurement of an unpainted section of RG-51 waveguide revealed an attenuation of approximately 0.02 db/ft. thus verifying that this difference is actually due to the zinc chromate.

Once the group velocity and the attenuation for a particular frequency and waveguide are known, the return loss for all discontinuities can be found by adjusting the measured apparent return loss, using equation (1).

In order to verify measurements taken by the pulse method, a low-loss movable load was constructed, which allowed a comparison of the load reflection coefficients (ρ) measured by both the slotted line and the pulse techniques. The load was obtained by applying a piece of reflecting

material to the absorbing cone of a movable matched-waveguide termination. Various foil shapes were tried in order to obtain a reasonably flat frequency response. The variation of the reflection coefficient with frequency, for the load finally used, is shown in Figure 15. The reflection coefficient is relatively constant for the pulse bandwidth of about 100 MHz centered at a frequency of 8.8 GHz.

The response law of the HP-423A detector, used for slotted-line measurements, measured 2.03 and resulted in a correction factor of 0.9896, which was calculated in accordance with reference 9. The measured VSWR is multiplied by this factor to correct for the detector's deviation from square-law response.

Since the load was movable, it was possible to separate the VSWR due to the load itself from the residual VSWR, due to fixed phase reflections from all other set-up discontinuities, by the following approximations:

$$\begin{aligned} \text{VSWR}_{\text{load}} &\cong \sqrt{\text{VSWR}_{\text{max}} \cdot \text{VSWR}_{\text{min}}} \\ \text{VSWR}_{\text{residual}} &\cong \sqrt{\frac{\text{VSWR}_{\text{max}}}{\text{VSWR}_{\text{min}}}} \end{aligned} \quad (2)$$

These approximations are derived in the appendix. The maximum and the minimum VSWR's were obtained by moving the load over several wavelengths. These approximations are very good when the measured VSWR's are small.

The movable load was measured with both slotted-line and pulse techniques on the test bench and again by pulse

technique when the load was mounted on the radar waveguide at a distance of 35.5 feet. The measurements were as follows:

Measurement Method	R_L min (db)	R_L max (db)	VSWR max	VSWR min	VSWR res	VSWR load
<u>Slotted line</u>			1.34	1.30	1.015	1.320
<u>Pulse</u>						
Bench	17.04	17.74	1.33	1.30	1.012	1.316
35.5'	15.06	19.90	1.43	1.226	1.082	1.322

Frequency of measurement: 8.80 GHz

Table 1. Sliding-load measurements.

A comparison of the slotted-line measurement with either of the pulse measurements shows a difference which is, however, within the accuracy of the precision attenuator. The maximum and minimum returns from the movable load at a distance of 35.5 feet down the waveguide are shown in Figure 16.

The residual VSWR for the 35.5 foot case is substantially larger than the residual VSWR for the bench measurement. This is expected due to the addition of a transition piece required to adapt the load to the waveguide.

These measurements verify that R_L can be measured with reasonable accuracy for a discontinuity some distance down the waveguide.

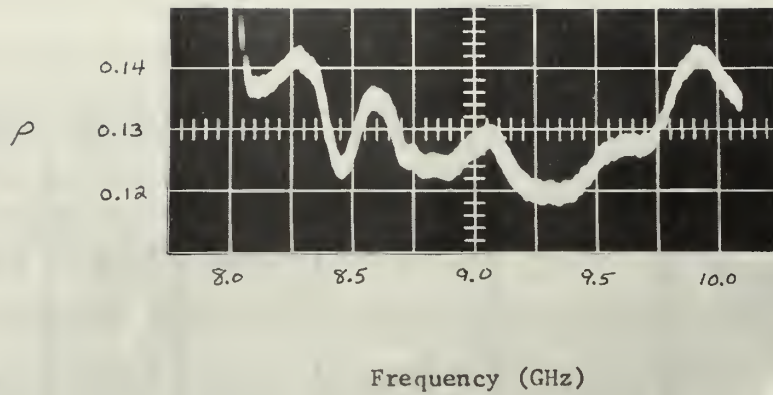
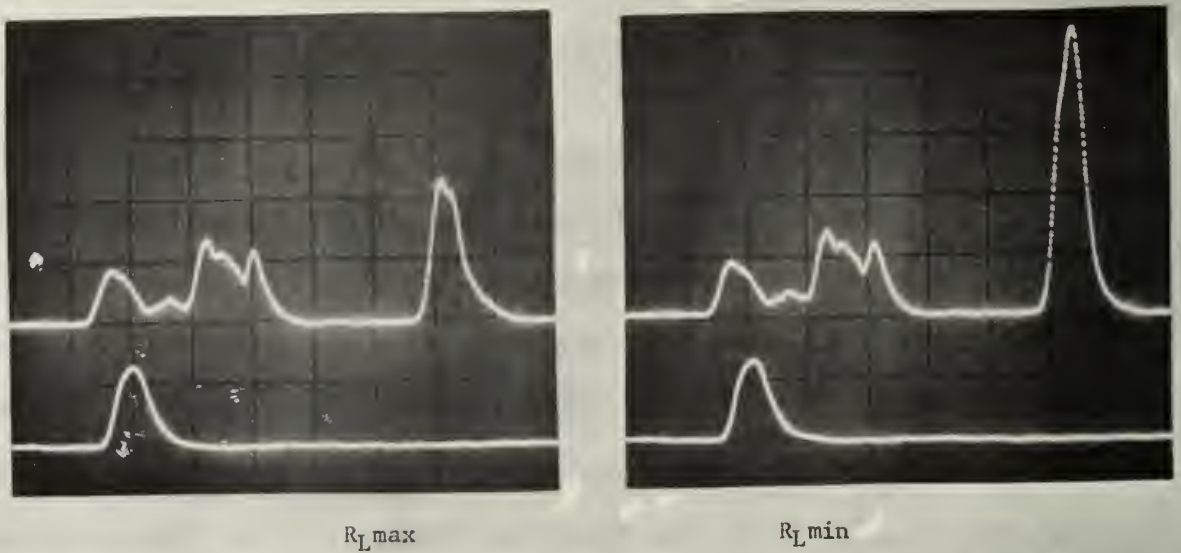


Figure 15. Moveable-load reflection coefficient versus frequency.



Scale: hor. 2ms/cm, vert. reflected r-f envelope at 50mv/cm.

Figure 16. Sliding-load reflections.

It is significant to note the inherent advantage of the pulse measurement system in terms of sensitivity. Conceivably it is possible to increase sensitivity to any desired level by increasing the peak pulse power. However the precision measurement of extremely small discontinuities is prevented by the inability to achieve attenuator readings for values of return loss above 50 db. Furthermore it is questionable whether higher sensitivities than those attained with just 2 watts (49 db of return loss $VSWR \approx 1.01$) are of particular usefulness.

CHAPTER IV

TEST SAMPLES

A. Mismatches Due to Differences in Internal Waveguide Dimensions Within the Allowable Tolerance

Bench testing of various waveguide components was undertaken in order to investigate the pulse system capabilities. Tests were conducted with X-band RG-52 waveguide having nominal inside dimensions of 0.400 by 0.900 inches and allowable tolerances of $\pm .003$ inches. Prior to the measurement of waveguide components it was desirable to get an idea of the reflections due to flange couplings alone. This was achieved by using a sliding termination as shown in Figure 17.

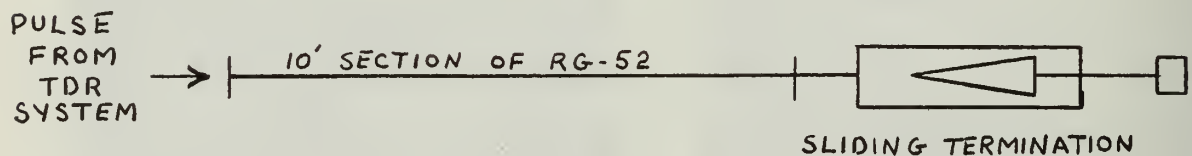
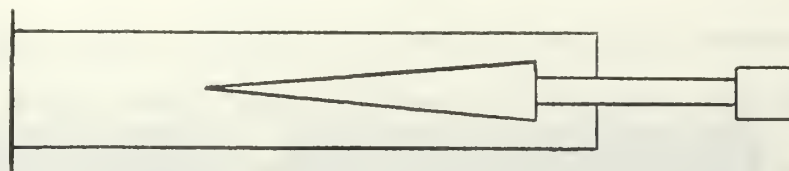
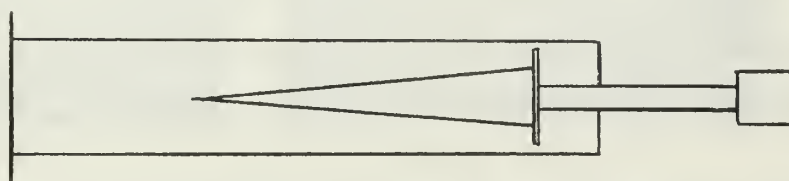


Figure 17. Coupling-return loss measurement.

The position of the load was varied for maximum and minimum reflected pulse amplitudes. Measurement of the return loss at these two positions allowed separation of the load-return loss from the residual return loss due to all fixed phase reflections within the pulse-resolution distance.



Termination number 1.



Termination number 2

Figure 18. Types of sliding termination.

The two types of sliding termination used are shown in Figure 18. In the first termination (Case I), the absorbing cone alone is moveable. In the second termination (Case II), however, the cone is mounted on the rear wall which in turn is moveable. Assuming that the changes in waveguide dimensions along any section are negligible, or so gradual as to have negligible return loss, the measured return losses are then assumed to have been caused by the flange coupling, the rear wall, and the sliding load. In Case I the fixed-phase discontinuities consisted of those from the coupling plus the rear wall. In Case II (since the rear wall was moveable), the flange coupling was the only source of fixed-phase reflections. For this reason the second case was expected to give very accurate measurement of the coupling loss alone. For Case III a measurement of the No. 1 termination was made

with a piece of reflecting foil having an area of two square millimeters, applied to the tip of the absorbing cone. The reflections obtained in each of the three cases are shown in Figures 19 through 21, and a summary of the above measurements is given in Table 2.

All measurements shown in Table 2 were made in decibels of return loss. This can be converted directly into voltage reflections coefficient (ρ) by the relationship:

$$R_L = -20 \log \rho \quad (3)$$

The residual reflection coefficient (ρ_R) combines with the load reflection coefficient (ρ_L) to yield:

$$\begin{aligned} \rho_{MAX} &= \rho_L + \rho_R \\ \rho_{MIN} &= \rho_L - \rho_R \text{ or } \rho_R - \rho_L \end{aligned} \quad (4)$$

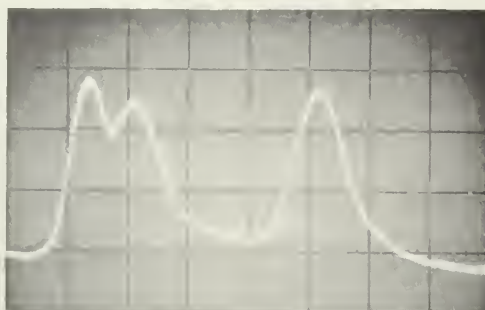
The load and residual reflection coefficients determined from the above are:

$$\begin{aligned} \rho_L \text{ or } \rho_R &= \frac{\rho_{max} + \rho_{min}}{2} \\ \rho_R \text{ or } \rho_L &= \frac{\rho_{max} - \rho_{min}}{2} \end{aligned} \quad (5)$$

The maximum theoretical values of return loss due to internal dimension differences for various waveguides are reported by A. F. Pomeroy in the Bell Laboratories Record.⁷ These values served as a basis for comparison with the actual measurements taken on the particular waveguide tested.



R_L max 45.00 db



R_L min 42.82 db

Figure 19. Case I Termination number 1, scale 10 ns/cm



R_L max 49.00 db



R_L min 40.35 db

Figure 20. Case II Termination number 2, scale 10 ns/cm.



R_L max 46.70 db



R_L min 42.60 db

Figure 21. Case III Termination no. 1 with reflection foil.

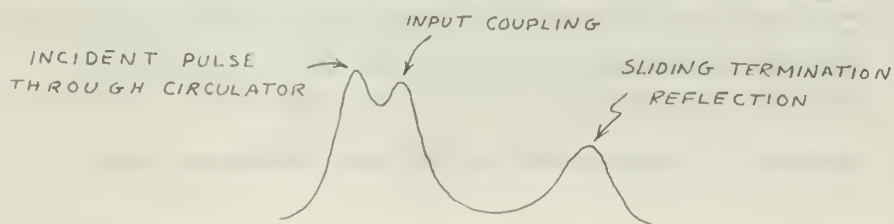


Figure 22. Load return legend.

	Case I	Case II	Case III
R_L max (db)	45.00	49.00	46.70
R_L min (db)	42.82	40.35	42.60
ρ min	.00562	.00354	.00462
ρ max	.00723	.00961	.00940
ρ residual	.00643	.00658	.00701
ρ load	.00080	.00303	.00239
R_L residual (db)	43.85	43.69	43.09
R_L load (db)	61.92	50.36	52.44
Dimen. Diff. (in.)	.0023	.0012	.0023
Max. Theo. R_L (db) (for given dimen. differ.)	40.0	45.8	40.0

Table 2. Summary of measurement results.

Dimensions (inches)	narrow	wide
10 foot section of RG-52	.3984	.9008
No. 1 sliding termination	.4007	.9010
No. 2 sliding termination	.3996	.8997

Inside dimensions measured by micrometer.

Table 3. Internal waveguide dimensions.

In Cases I and III, the residual return loss is determined largely by the coupling discontinuity as modified by the rear wall return. As pointed out, however, in Case II the residual return loss is determined completely by the coupling, since it is the only fixed source of reflection. In this case the maximum dimension difference is 0.0012 inches in the narrow dimension. The maximum theoretical return loss given by Pomerooy for this difference in RG-52 is 45.8 db. This means that for a difference in internal dimensions of 0.0012 inches, the reflected power will be no more than the maximum theoretical return loss. The measured value of return loss equal to 43.69 db is reasonable in that it does not exceed the maximum theoretical value.

In Cases I and III the measured residual return losses were 43.85 and 43.09. These are as close to each other as expected, but exceed the maximum theoretical value for a difference in dimension of 0.0023 inches. This is due to the interaction of the rear wall and the flange reflections which cancel each other and give a lower return loss. It is worth noting that in Case III, the addition of a 2-square-millimeter piece of reflecting material caused a decrease in the load-return loss of about 9.5 db, thereby positively identifying it as the loss due to the load. The micrometer readings are accurate to about ± 0.0003 inches and the precision attenuator readings to $\pm 2\%$ of the db scale readings. This amounts to a variation in either the maximum theoretical value of return loss or the measured return loss of about ± 1 db.

The maximum possible difference in dimensions within the allowable tolerances is 0.006 inches and gives a maximum theoretical return loss for RG-52 of 31.5 db. This corresponds to a VSWR of about 1.055 and indicates the range of mismatch which can be expected just from differences in waveguide dimensions within the manufacturers' tolerances.

B. Reflections from Various Waveguide Components.

The bench set-up used for testing waveguide components is shown in Figure 23. The reflection received from this set up with no test component is shown in Figure 24. The pulse shown is the incident pulse through the circulator, 43 db down.

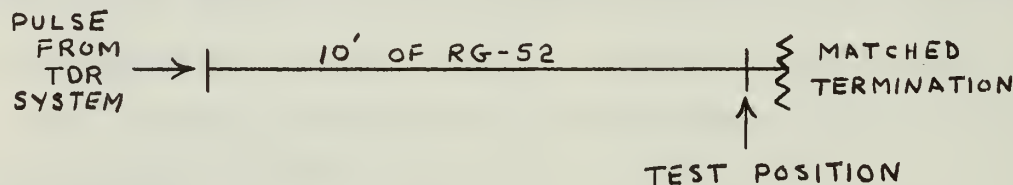


Figure 23. Bench set-up.

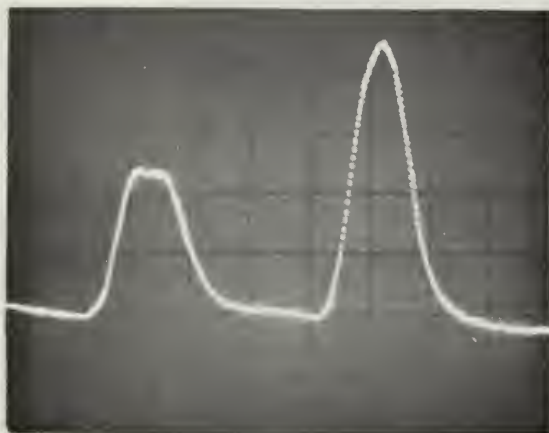
Figures 25 through 29 show reflections from various waveguide components using this set-up. The reflection shown in Figure 21 is due to a matched termination, the narrow dimension of which is 0.0015 inches undersize compared to the termination used in the basic set-up. The theoretical return loss for such a dimensional difference is about 44 db, which compares closely.

The return loss due to the choke coupling shown in Figure 29 represents a transmission loss of only 0.00043 db. This is much lower than that listed in Microwave Transmission Design Data, which gives the transmission loss for a brass choke and flange joint at x-band in the range of 0.009 to 0.013 db.⁸



Scale: 10 ns/cm
5 mv/cm
Frequency: 8.86 GHz

Figure 24. Reflection without test component.



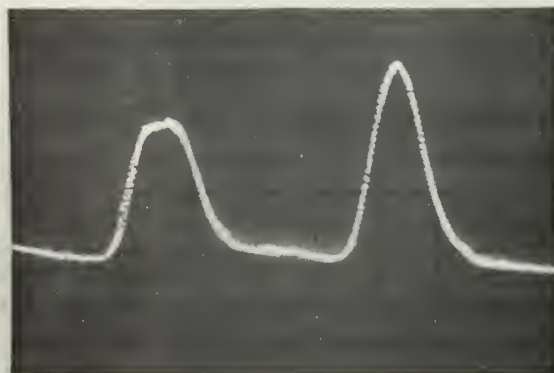
Scale ns/cm
 $R_L = 39.45$ db
VSWR = 1.023

Figure 25. 90 degree twist



Scale: 10 ns/cm
 $R_L = 46.4$ db
VSWR = 1.01

Figure 26. Matched termination. (.0015" undersize)



Scale: 10 ns/cm
 $R_L = 41.15$ db
 VSWR = 1.018

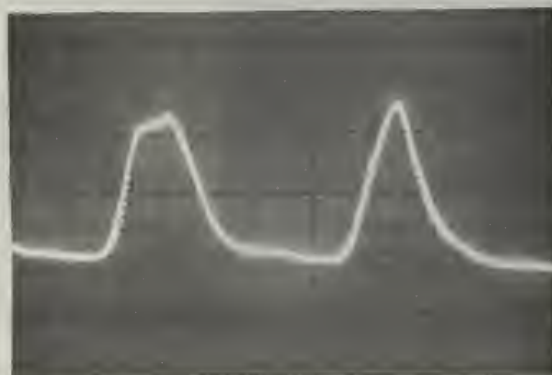
Figure 27. 90-degree E bend.



Scale: 10 ns/cm
 Frequency: 8.86 GHz
 $R_L = 37.8$ db
 VSWR = 1.028

Note: This E bend has a turning radius about 1/3 that of the bend shown in Figure 27.

Figure 28. 90-degree E bend.



Scale: 10 ns/cm
 Frequency: 8.86 GHz
 $R_L = 42.0$ db
 VSWR = 1.016

Figure 29. Flat flange to choke flange connection.

C. Variation of Propagation Velocity and Attenuation with Frequency

The set-up in Figure 30 was used to demonstrate the variations of attenuation and group velocity with frequency for RG-52 waveguide. The pulse from the TDR system is sent into the arm of the 10-db directional-coupler. It is then reflected back and forth between the shorts on either end of the 11 foot 7 inch waveguide section. Each reflection from the distant short is detected and displayed as shown in Figure 31.

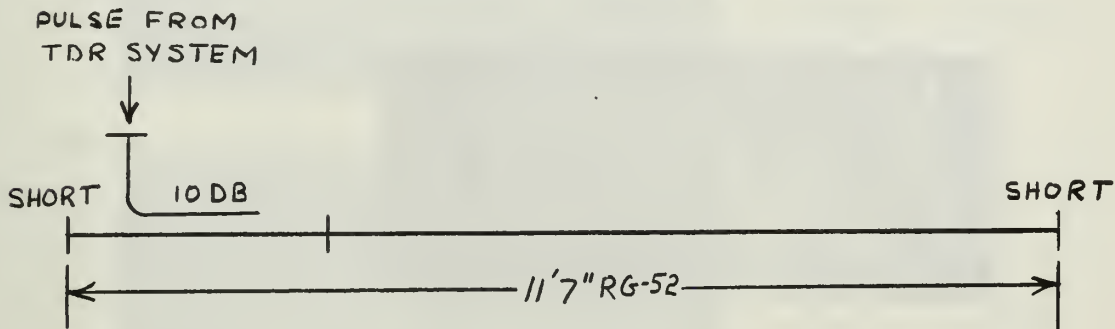
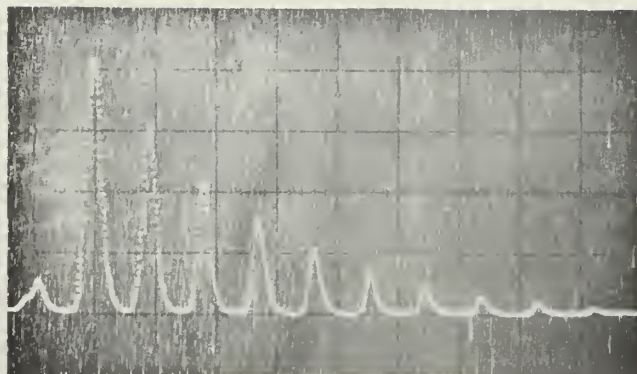


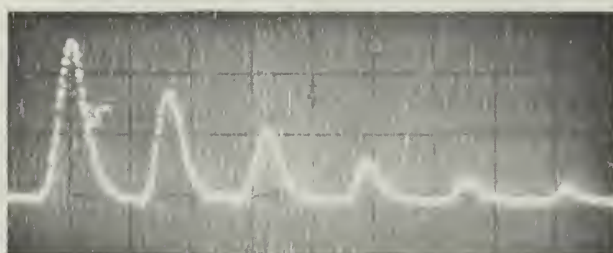
Figure 30. Set-up for RG-52

The reflections received at various frequencies starting with the highest are shown in Figure 32. In this sequence of photographs the decrease in group velocity can be seen as an increase in the time between reflections. The damping of the pulse sequence in each case is caused in approximately equal measure by the two-way transmission loss of the coupler and the waveguide attenuation. However, the effect of the changing waveguide attenuation with frequency can be observed as a decrease in amplitude of corresponding reflections.

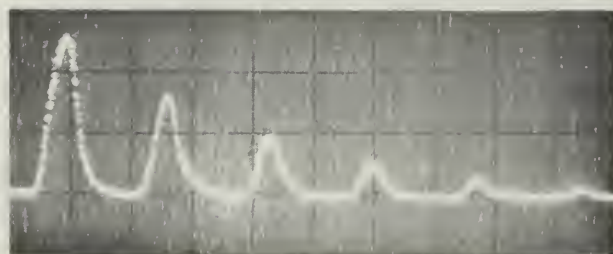


Scale: 40 ns/cm
Frequency: 8.86 GHz

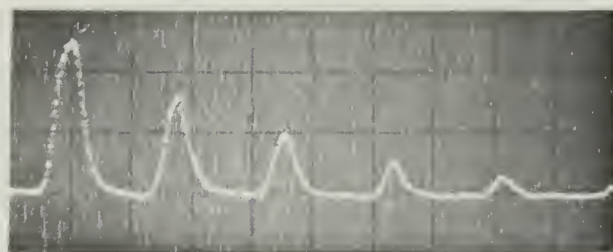
Figure 31. Multiple reflections from shorted waveguide section.



Frequency: 10.01 GHz

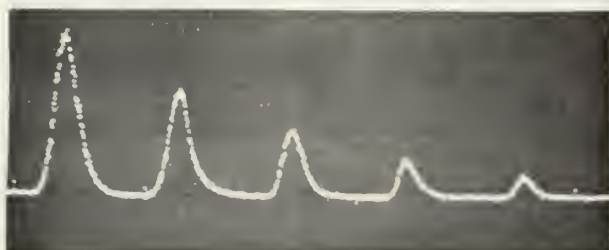


Frequency: 9.4595 GHz



Frequency: 9.005 GHz

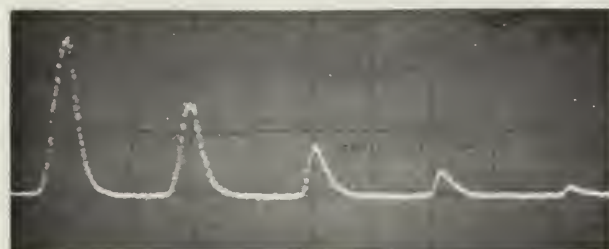
Figure 32. Variation of attenuation and propagation velocity with frequency.



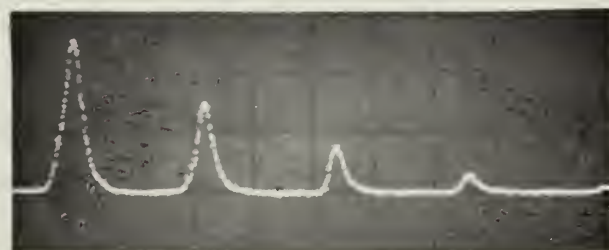
Frequency: 8.596 GHz



Frequency: 8.247 GHz



Frequency: 8.06 GHz



Frequency: 7.88 GHz



Frequency: 7.10 GHz

Figure 32. (continued)

D. Delay Distortion

One effect due to the wide bandwidth of the pulse used with the TDR system is the distortion of the pulse after traveling a distance in the waveguide. This occurs because the high-frequency components of the pulse travel faster than the low-frequency components, eventually causing pulse distortion. The equation relating the factors which determine the modulating bandwidth causing a specified amount of distortion is given by A. E. Karbowiak¹⁰ as:

$$BW = 19.5 \left(\frac{f}{f_c} \right) \left(\frac{f}{L} \right)^{\frac{1}{2}} (\delta \phi)^{\frac{1}{2}} \quad (6)$$

where:

BW = double side bandwidth in MHz

f = carrier frequency in GHz

f_c = cut-off frequency in GHz

L = length of waveguide in kilometers

δφ = permissible differential phase delay between the carrier and the sidebands, in radians

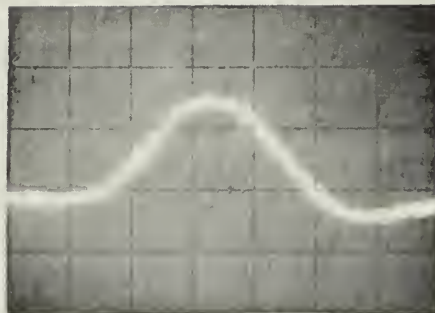
The permissible amount of delay distortion (δφ) is a function of modulation method. For example, in the case of a single frequency, amplitude-modulated signal, a relative phase error of 90 degrees ($\delta \phi = \frac{\pi}{2}$) would cause conversion of amplitude modulation to phase modulation. For pulse-modulation methods on the other hand, the permissible value of δφ is about one radian. This value of permissible delay, when applied to the TDR pulse system for a particular

waveguide, would give the maximum usable pulse bandwidth. For 100 feet of RG-51 at a frequency of 8.8 GHz, the maximum bandwidth is about 400 megahertz. This means that for this particular case, a r-f pulse of a width as narrow as 2.5 nanoseconds could be used, giving a resolution to within one foot.

An attempt was next made to observe the delay distortion of the pulse employed by the TDR system. The set-up shown in Figure 30 was again used with RG-52 waveguide. This waveguide was smaller than that of the other systems tested and therefore had narrower permissible bandwidth for a given length. The pulse was sent into the 11-foot 7-inch section of shorted waveguide and the echo most distant in time was inspected for distortion. In this case, it was possible to view the 10th-time-around reflection. This gave an equivalent waveguide length of over 200 feet and permitted a bandwidth of about 300 megahertz. The first and tenth reflections are shown in Figure 33.

In order to achieve faster detection response, the crystal was terminated with 25 ohms instead of 40 ohms, thus accounting for the overshoot at the trailing edge of the pulse.

The general effect of delay distortion is a spreading in time of the energy of the main body of the pulse. In the case shown, no spreading was noticeable; in fact, the pulse appeared narrower after the tenth round trip. Spreading was not expected because the effective system bandwidth



1st Return

9.44 GHz

Scale: 4ms/cm



10th Return

Figure 33. Delay distortion.

was 300 MHz and the pulse used was on the order of 10 ns with a bandwidth of 100 MHz. The reasons for the pulse becoming narrower after traveling about 200 feet were not completely determined.

As far as delay distortion is concerned, the existing conditions would permit a much narrower pulse; however, in practice, a 10 nanosecond pulse with 4-foot resolution is quite satisfactory for locating faults to within one flanged waveguide section, since sections usually are 10 feet long.

E. Radar Waveguide System Tests

Three radar-waveguide systems installed at the Naval Postgraduate School were tested using the microwave TDR system. Each installation is longer than it would normally be under actual shipboard installation conditions. This proved to be helpful in providing a larger number of discontinuity samples than would ordinarily be available.

The first system to be tested was the SS radar waveguide. Figure 35 shows the reflections received at a test frequency of 8.80 GHz. These reflections are shown with an expanded time scale in Figure 36. A diagram of the installed system is given in Figure 34. The locations of discontinuities causing the reflections shown in Figures 35 thru 39 are indicated on the system diagram of Figure 34. Using the procedures outlined in Chapter III the apparent return loss of each discontinuity was measured and adjusted for two-way attenuation in order to find the return loss at the point of

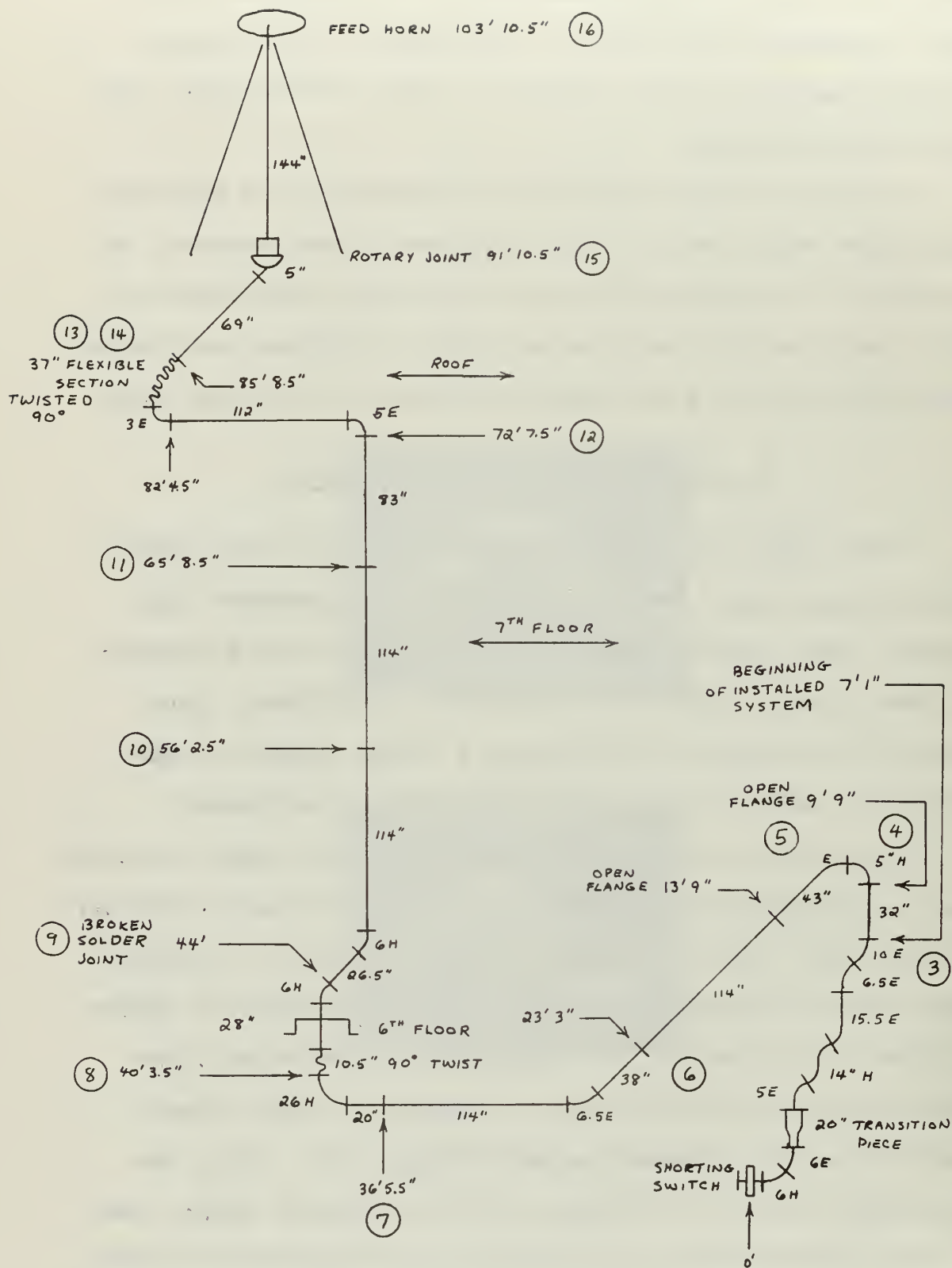
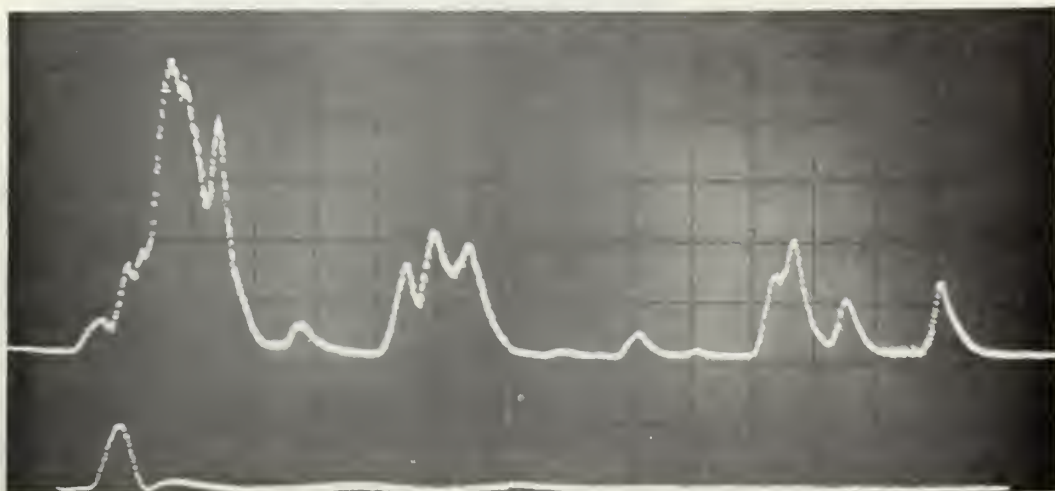


Figure 34. SS radar waveguide installation.

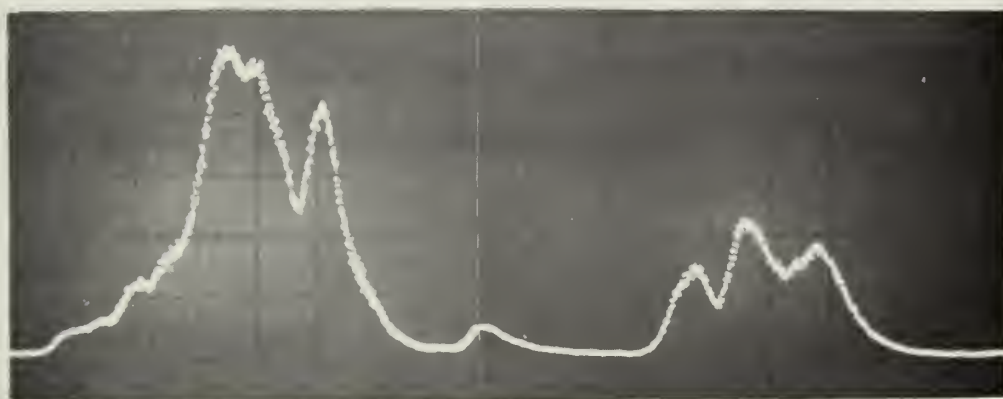


Scale: 20 ns/cm

50mv/cm

Frequency: 8.80 GHz

Figure 35. SS radar waveguide reflections.



Scale: 10 ns/cm

50 mv/cm

Frequency: 8.80 GHz

Figure 36. SS radar waveguide reflections,
expanded time scale.

discontinuity. Table 4 lists the readings taken, the adjustments for attenuation, and the final return loss for each discontinuity. For this waveguide system, as well as those following, the transmission losses of the intervening discontinuities were small enough to be omitted.

In order to compare the total waveguide transmission loss due to faults with the total waveguide attenuation, the individual transmission losses were found to total 0.0883 db. This compares with waveguide attenuation of 4.01 db. Together these make up the total waveguide loss of about 4.10 db. Based on these values, the overall transmission efficiency is 39 percent. If every fault were corrected completely, this would represent not more than a one-percent improvement in the transmission efficiency of the system. This illustrates the sensitivity of such a TDR system as a means of locating faults.

Figure 40 shows the reflections at 8.8 GHz, with VSWR curves plotted. These curves take into account waveguide attenuation and detector response. Since measurement of the detector response required tuning for different power levels, these VSWR curves are only approximate, but are included to show the variation of VSWR with distance as seen on the oscilloscope. It would conceivably be possible, however, to make a transparent overlay for a particular fixed-tuned radar system based on one scale setting. This scale setting could be calibrated by using the shorting switch and then used to read VSWR, or return loss due to

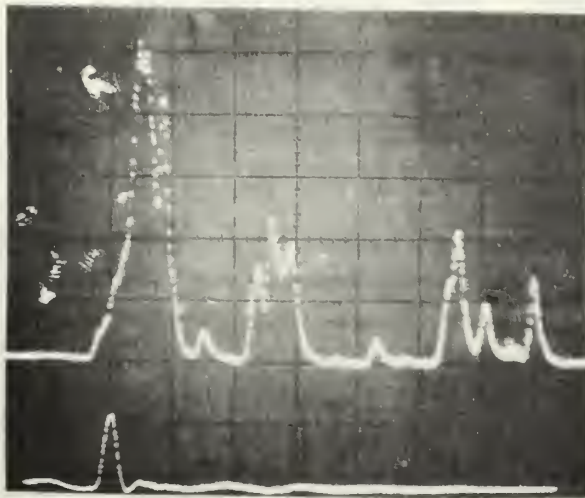


Figure 37. SS radar
waveguide reflections

Scale: 40 ns/cm

Frequency: 8.8 GHz

$v_g/2 = .380$ ft/ns

$a = .0386$ db/ft

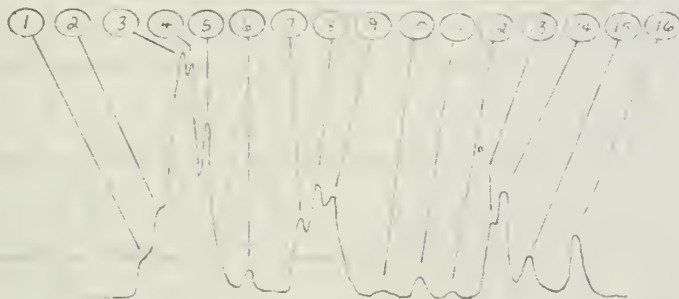


Figure 38. Legend for
SS waveguide reflections.

No.	t (ns)	d (ft)	L_{Rapp} (db)	$2a_1$ (db)	L_R (db)	VSWR	L_T (db)
1	isolation		38.80				
2	4	1.0	34.64	.08	34.56	1.040	.0017
3	18	7.0	25.50	.54	24.96	1.118	.0140
4	24	9.0	25.88	.70	25.18	1.116	.0130
5	29	11.0	26.97	.85	26.12	1.104	.0110
6	60	22.8	39.65	1.76	37.89	1.030	.0010
7	95	36.0	33.79	2.78	31.01	1.060	.0036
8	103	39.0	31.58	3.00	28.58	1.078	.0062
9	114	43.5	32.55	3.36	29.19	1.072	.0053
10	149	56.5	47.00	4.36	42.64	1.020	.0004
11	174	66.0	41.52	5.10	36.42	1.033	.0013
12	195	74.0	47.00	5.71	41.29	1.020	.0004
13	218	83.2	35.10	6.43	28.67	1.078	.0062
14	224	85.2	32.00	6.58	25.42	1.113	.0120
15	242	92.0	37.30	7.10	30.20	1.064	.0042
16	274	104.0	35.50	8.00	27.50	1.087	.0080
							<u>.0883</u>

Transmission Loss .09
 Attenuation (104 x .0386) 4.01
 Total Waveguide Loss 4.10 db
 Waveguide Efficiency = 39%

Table 4. SS waveguide measurement data.

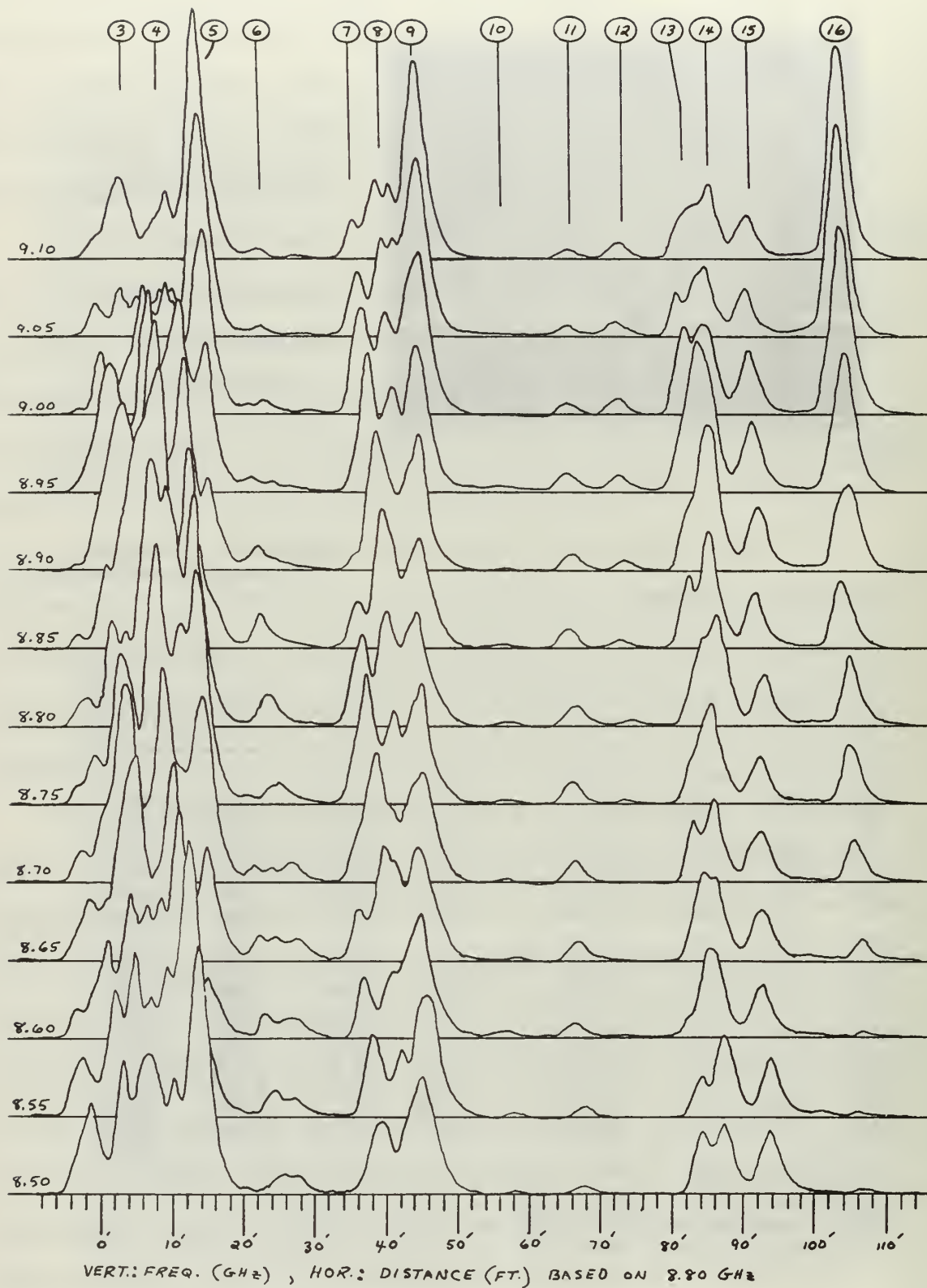


Figure 39. SS radar waveguide reflections at frequencies 8.5-9.1 GHz.

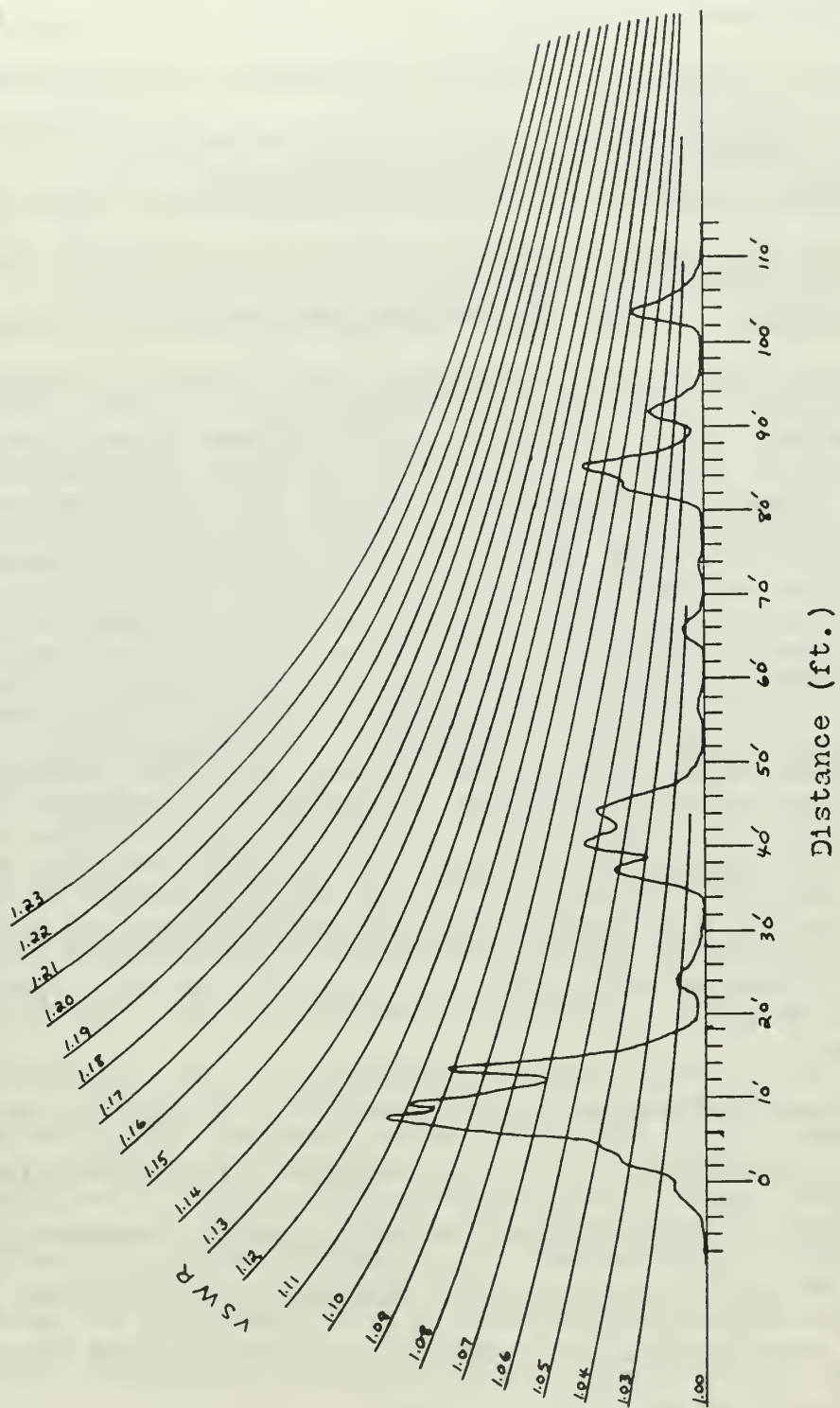


Figure 40. SS radar waveguide reflections at 6.3 GHz.

individual discontinuities directly off the oscilloscope.

For a broadband or tunable system this technique would not be useful since the curves are only good for one value of waveguide attenuation and group velocity. In this case, a series of displays such as are shown in Figure 39, showing the frequency dependency of the discontinuities, would be more helpful in locating trouble spots. The distance scale for this figure is based on the group velocity at a frequency of 8.80 GHz. For other frequencies there exists a slight distance error, which increases with distance along the guide and frequency deviation from 8.80 GHz. As frequency is increased above 8.80 GHz, the group velocity increases and the return echoes occur earlier in time. Based on the 8.80 GHz distance scale, these returns also appear to come from a closer point on the waveguide. The same effect occurs in the opposite sense as frequency is decreased below 8.80 GHz. In figure 39, the maximum shift due to this effect is equivalent to 1.5 feet in 100 feet and is seen as a shifting of the distance reflections to the left at the higher frequencies.

As a means of comparing the results obtained by the TDR system with those which would be obtained by slotted-line or directional-coupler SWR measurement, swept-frequency methods were used to measure the reflection coefficient for the three radar waveguides tested. The set-up used for these measurements is shown in Figure 41.

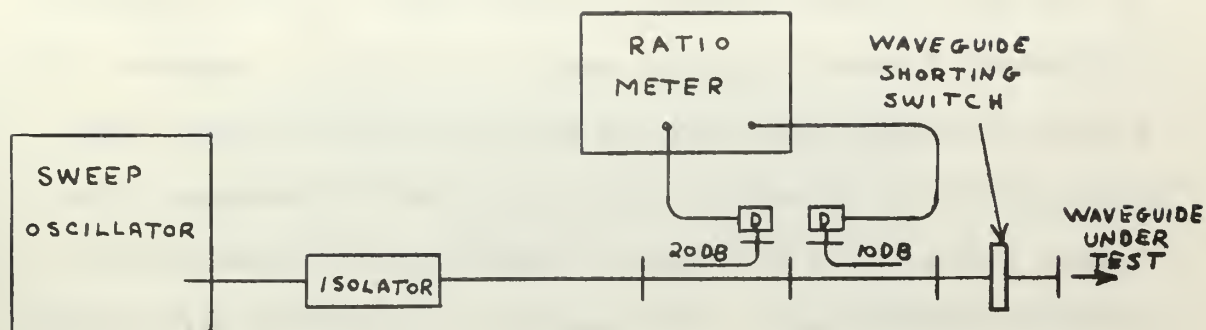


Figure 41. Swept-frequency measurement of reflection coefficient.

The plots of the reflection coefficient versus frequency for successively narrower sweep bandwidths are shown in Figure 43. These correspond to the SWR which would be measured by slotted-line or directional-coupler techniques. Note that the general trend of the reflection coefficients is upward with increasing frequency from 8.80 GHz. This is in agreement with the general trend of the amplitudes of the echoes using the TDR method. In this case the slotted-line method of measurement is very sensitive to frequency.

The measurement of waveguide-system reflection coefficient with swept frequency techniques (frequency-domain reflectometry) is not practical for the location of faults in the waveguide systems tested. For the simple case of a waveguide with only two discontinuities of equal magnitude separated by a given distance, the variation of VSWR with frequency is periodic, with a cycle which depends on the separation distance and the frequency sweep rate. As the frequency is changed the VSWR will become minimum whenever an odd number of half-wavelengths equals the separation distance. In this case it is possible to find the location

of the two discontinuities by measurement of the frequency difference between adjacent maxima or minima. However, for a more realistic case such as the waveguides tested, the multiplicity of discontinuities produces VSWR-versus frequency plots which are almost impossible to interpret for distance information. For example, it would be very difficult to evaluate the plots of VSWR versus frequency shown in Figure 43 to determine the location of the corresponding waveguide discontinuities shown in Figures 35 through 37. Therefore, for actual waveguide installation fault-finding, frequency-domain techniques are not as useful as TDR methods.

The two additional X-band systems tested using time-domain reflectometry techniques were the Mark-25 and the Mark-13 radar waveguide installations. Results on both of these waveguide systems are reported in the same manner as the SS radar waveguide. Mark-13 waveguide data is contained in Figures 45 through 51 and Mark-25 waveguide data in Figures 52 through 58. The circled numbers on all figures refer to corresponding discontinuity locations.

Up to this point all tests were carried out at X-band. With the same techniques, similar testing was next attempted at L-band using the set-up shown in Figure 44. The reflections received from the SPS-6C surface-search-radar waveguide installation are shown in Figure 59. In this case, due to lack of time, no attempt was made to measure the returns from the discontinuities.

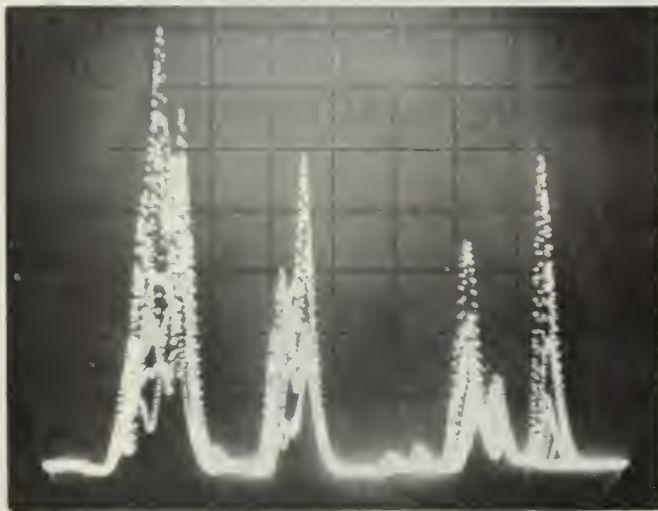


Figure 42. Multiple exposure of SS radar waveguide reflections from 8.5-9.1 GHz in 50 MHz steps.

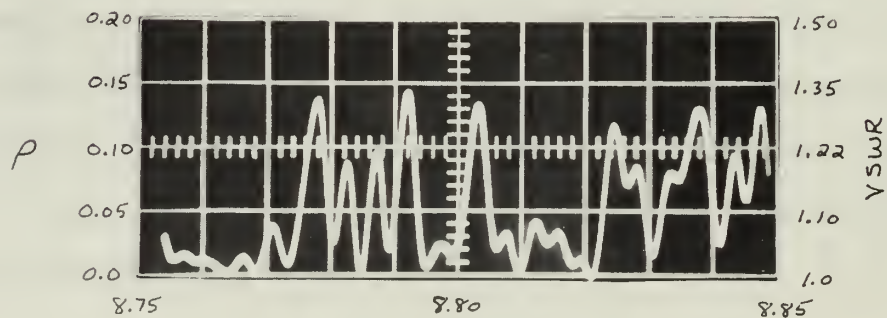
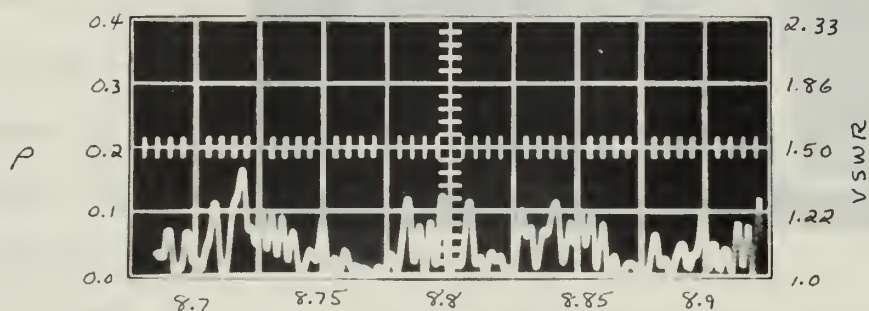
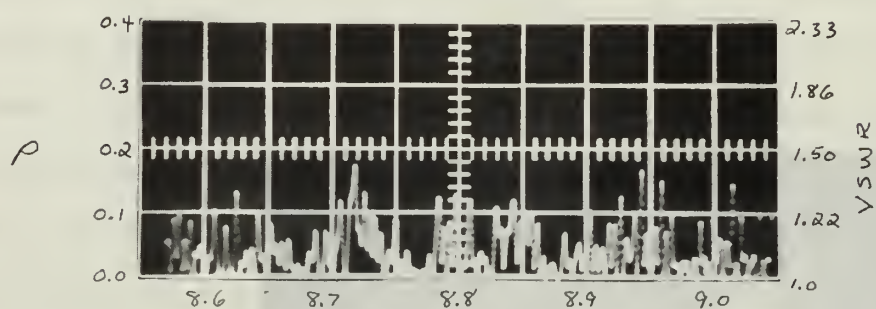
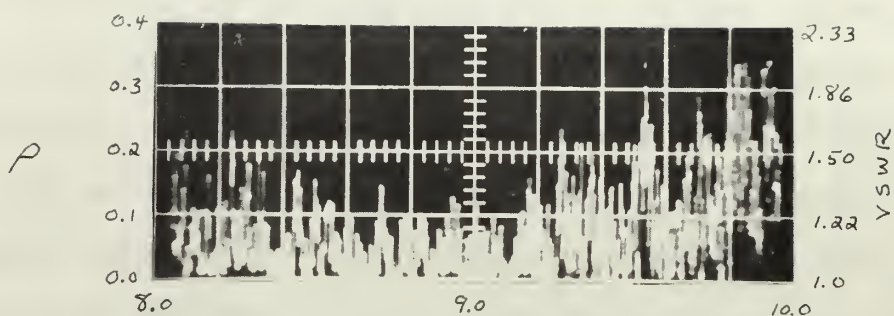


Figure 43. Voltage reflection coefficient versus frequency for SS radar waveguide.

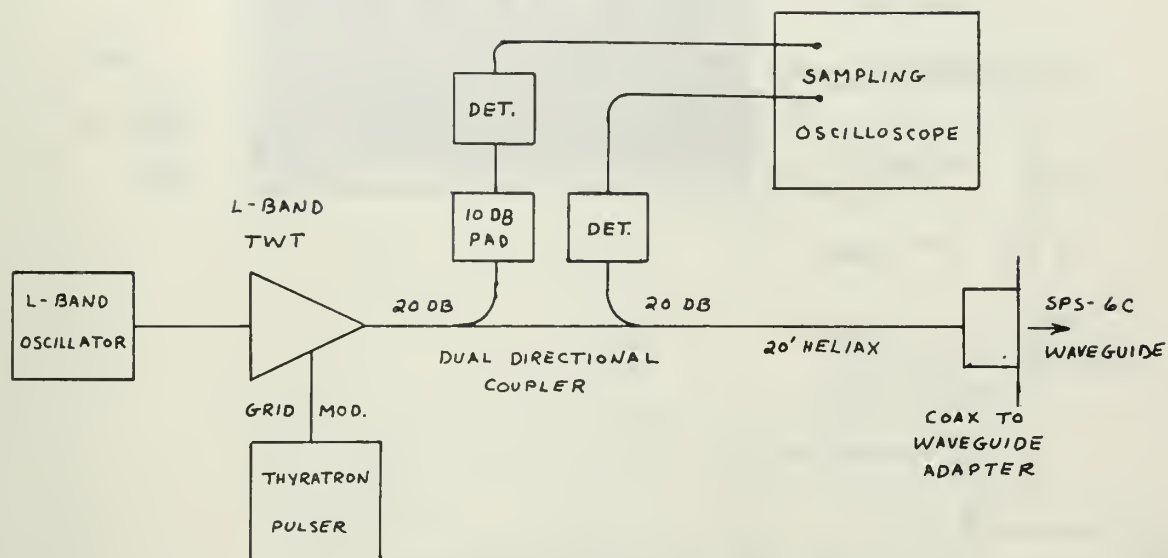


Figure 44. L-band test set-up.

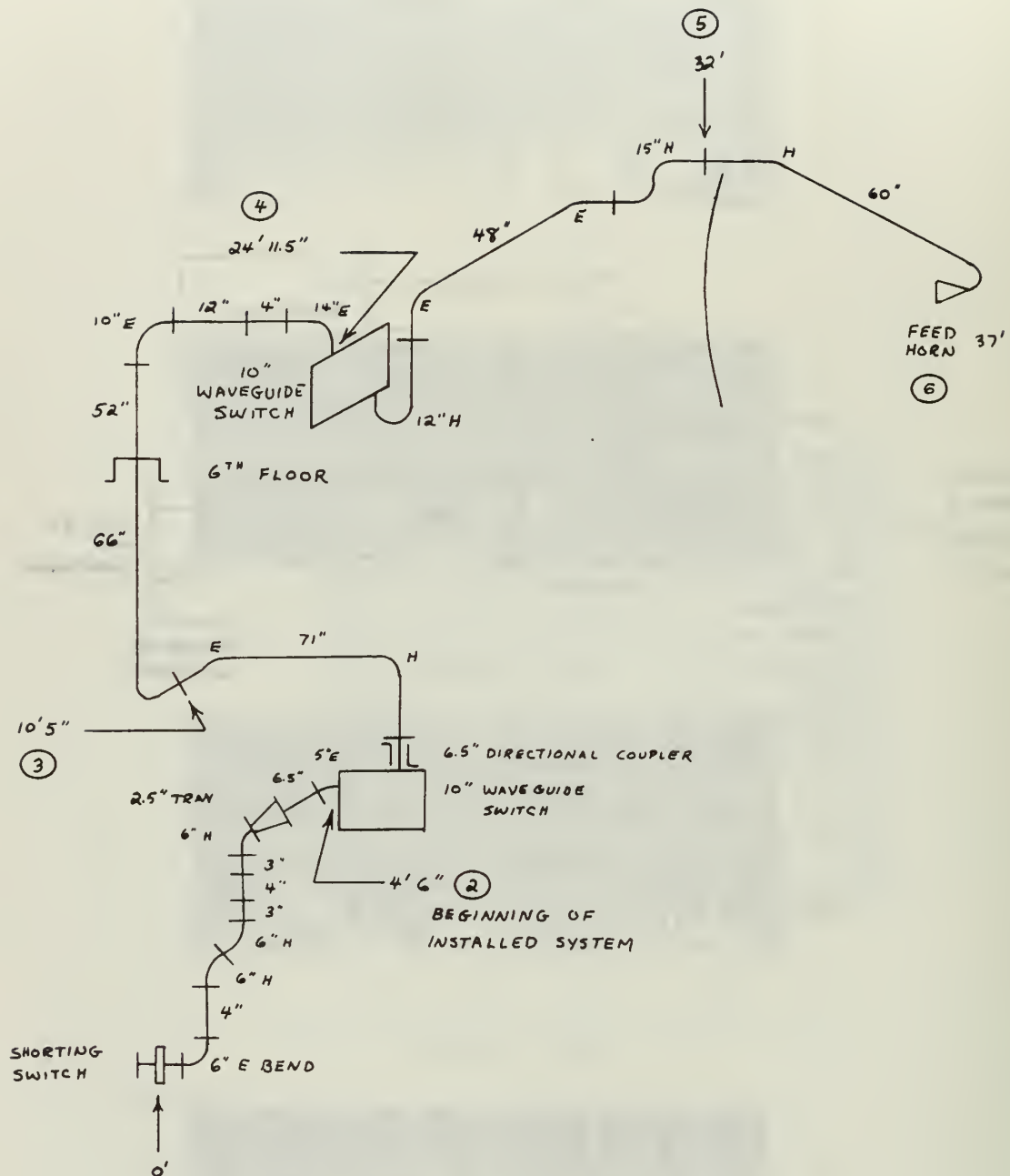


Figure 45. Mk 13 radar waveguide installation.

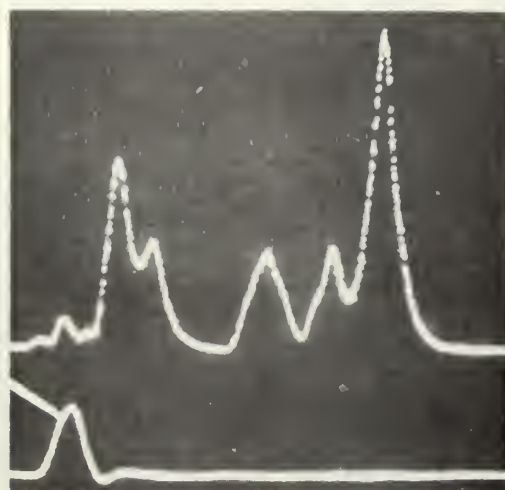


Figure 46. MK 13 radar waveguide reflections.

Scale: 20 ns/cm

Frequency: 8.8 GHz

$V_p/2 = .380$ ft/ns

$a = .0386$ db/ft

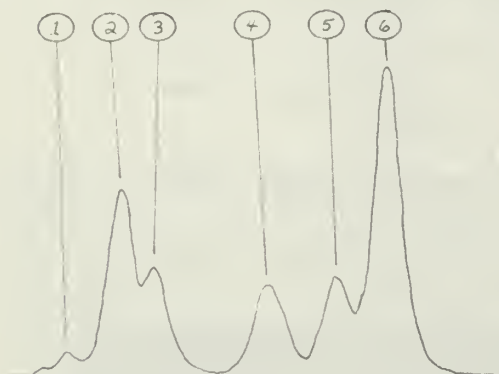


Figure 47. Legend for MK 13 radar waveguide reflections.

No.	t (ns)	l (ft)	L_{Rapp} (db)	$2a l$ (db)	L_R (db)	VSWR	L_T (db)
1	isolation		37.30				
2	16	6	26.80	.46	26.34	1.101	.0100
3	28	10.5	30.43	.81	29.62	1.068	.0047
4	63	24	31.40	1.85	29.55	1.069	.0050
5	85	32	31.00	2.47	28.53	1.078	.0062
6	100	38	23.30	2.94	20.36	1.213	<u>.0405</u>
							.0664

Transmission Loss .07
 Attenuation ($38 \times .0386$) 1.47
 Total Waveguide Loss 1.54 db
 Waveguide Efficiency = 70%

Table 5. MK 13 waveguide measurement data.

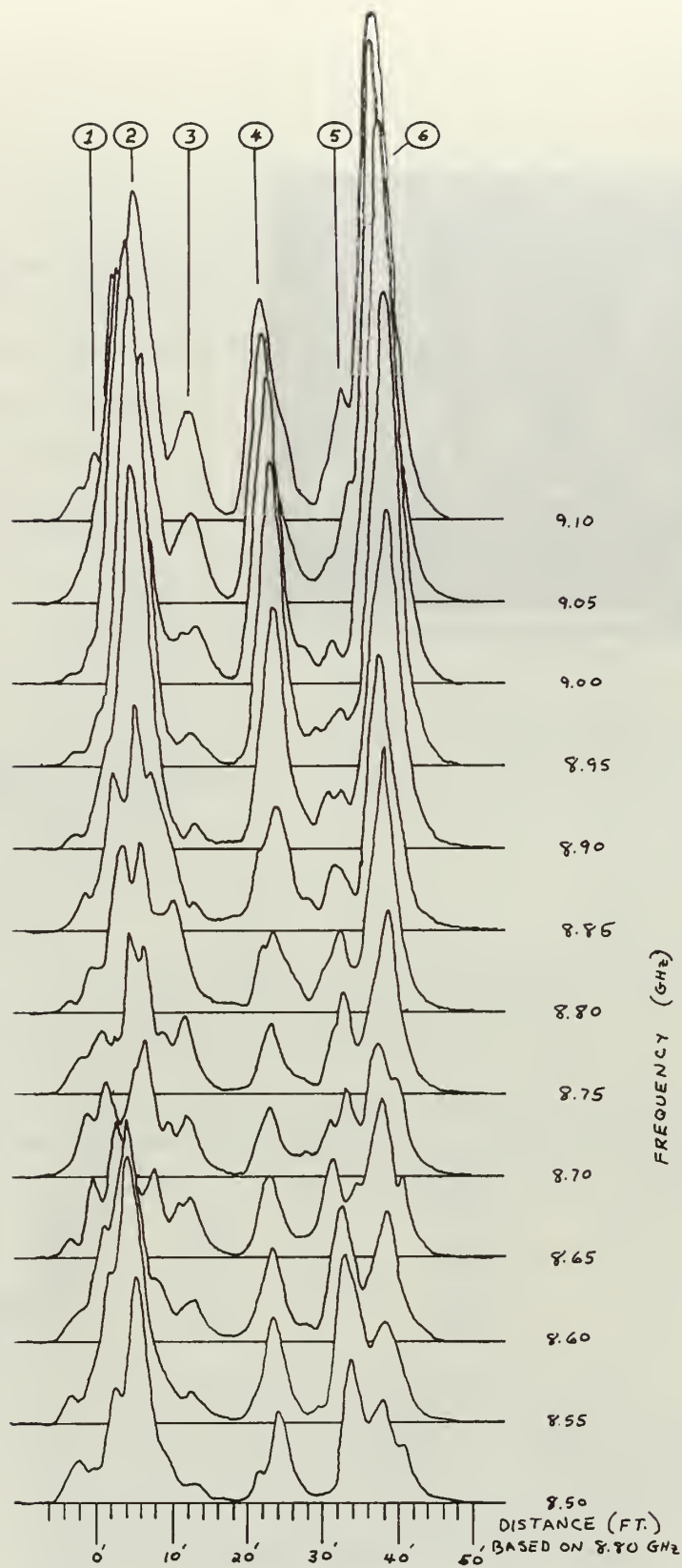


Figure 48. M-13 radar waveguide reflections at frequencies 8.5-9.1 GHz.

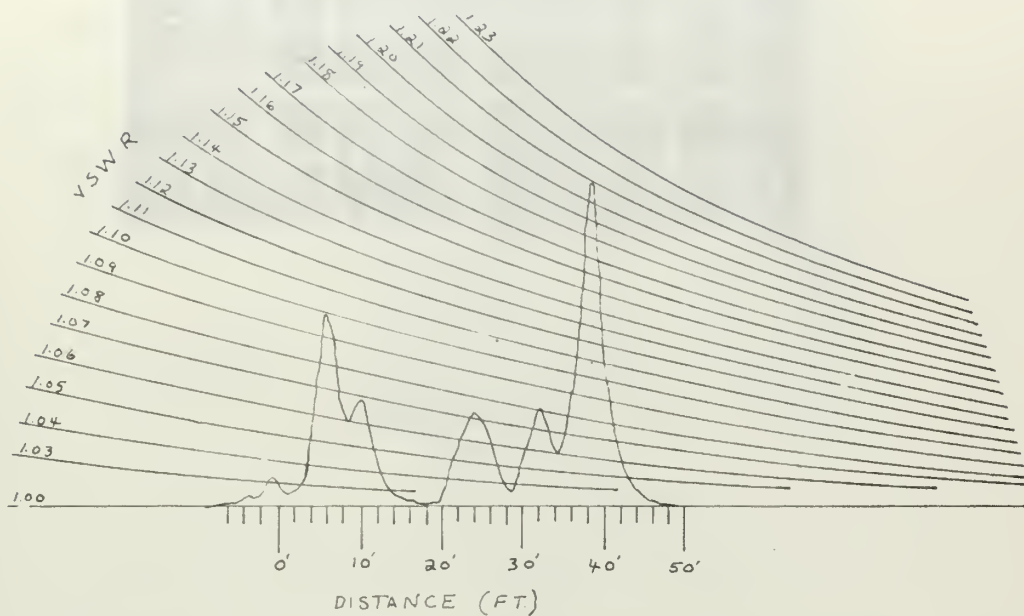


Figure 49. MK 13 radar waveguide reflections at 8.80 GHz

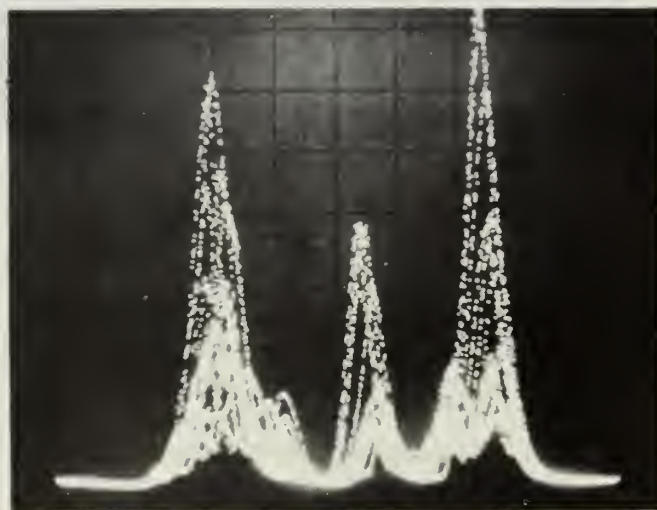


Figure 50. Multiple exposure of MK radar waveguide reflections at 8.5-9.1 GHz in 50 MHz steps.

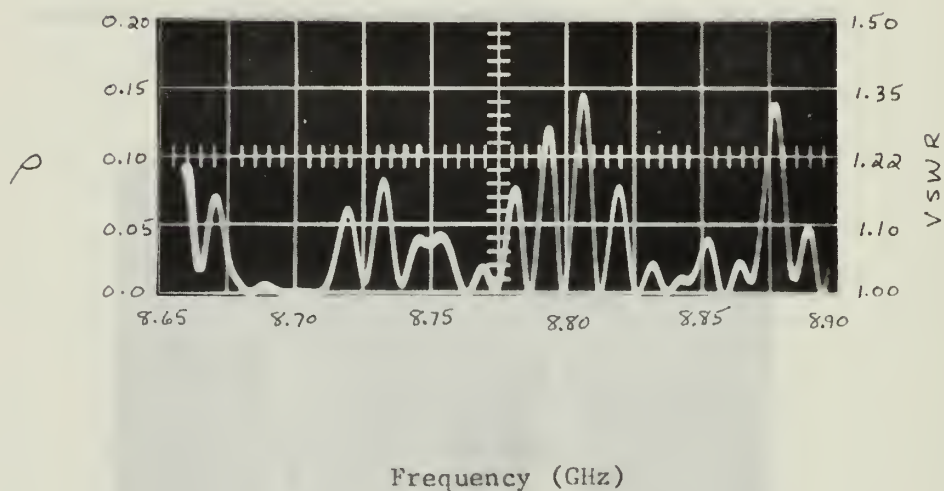
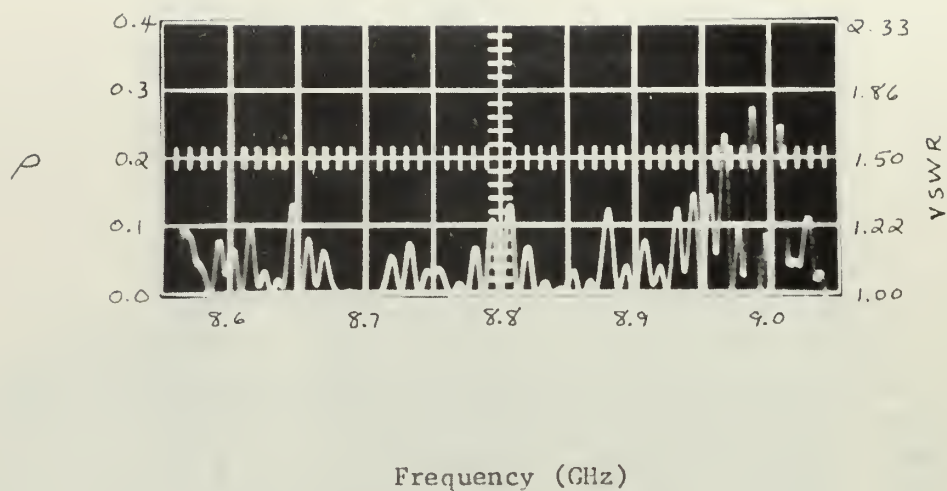


Figure 51. Voltage-reflection coefficient versus frequency for MK 13 radar waveguide.

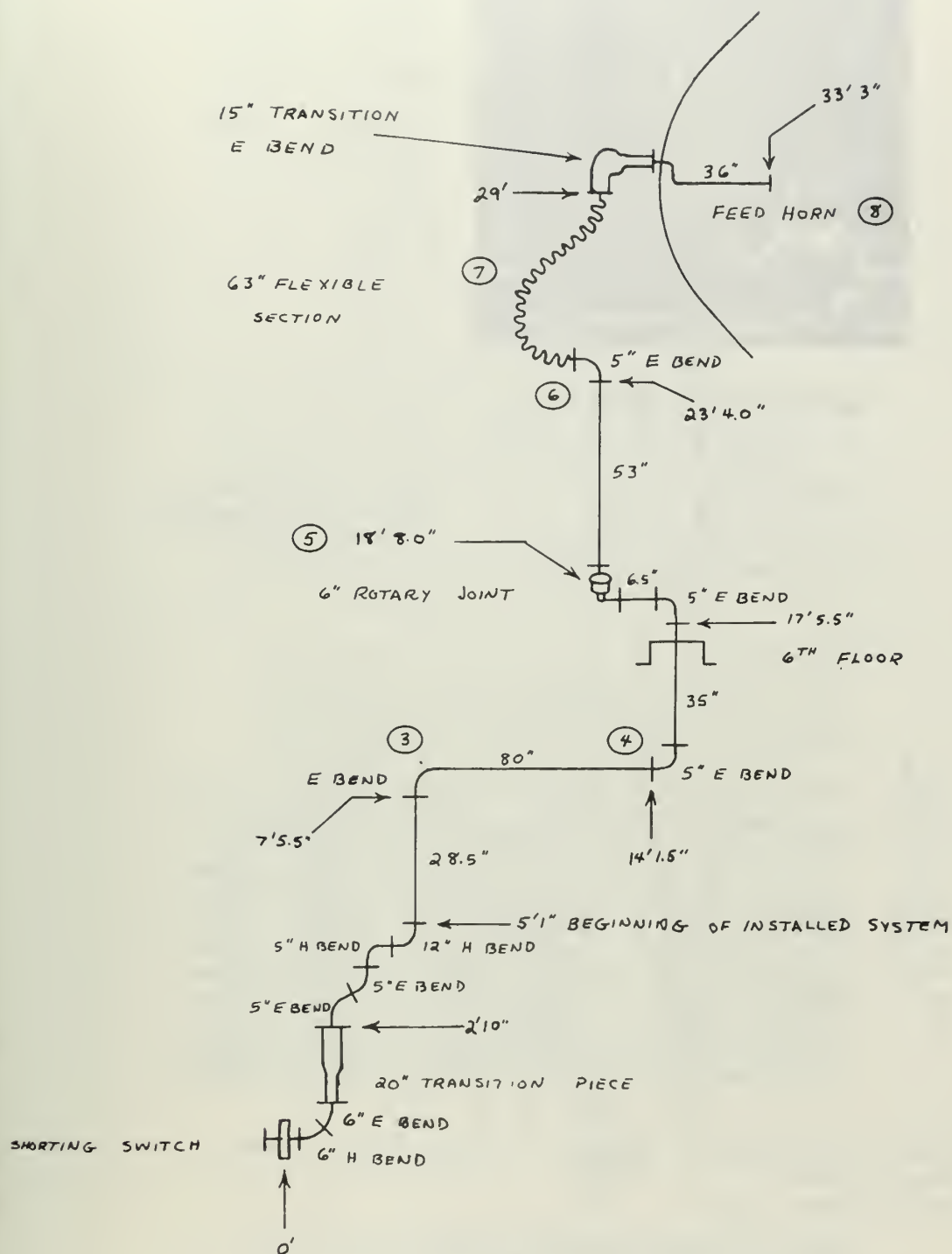


Figure 52. MK 25 radar waveguide installation.

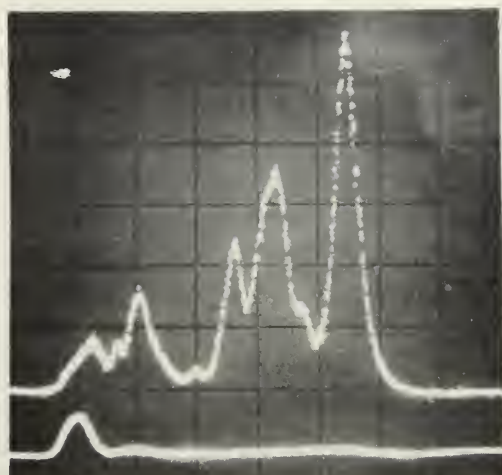


Figure 53. MK 25 radar waveguide reflections.

Scale: 20 ns/cm

Frequency: 9.10 GHz

$V_p/2 = .388$ ft/ns

$a = .0372$ db/ft

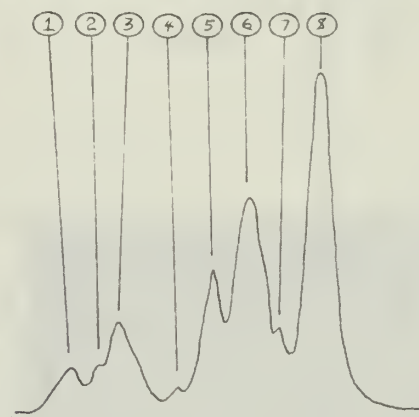


Figure 54. Legend for MK 25 radar waveguide reflections.

No.	t(ns)	l(ft)	L_{Rapp} (db)	2al(db)	L_R (db)	VSWR	L_T (db)
1	4	1.5	33.55	0.11	33.44	1.043	.0021
2	12	4.5	34.30	0.33	33.97	1.040	.0019
3	20	8.0	30.40	0.60	29.80	1.067	.0047
4	36	14.0	36.84	1.04	35.80	1.034	.0014
5	48	18.5	28.10	1.38	26.72	1.097	.0096
6	62	24.0	25.60	1.79	23.81	1.140	.0188
7	70	27.0	31.20	2.01	29.19	1.072	.0056
8	86	33.0	22.50	2.46	20.04	1.220	.0435
							<u>.0876</u>

Transmission Loss .09
 Attenuation ($33 \times .0372$) 1.23
 Total Waveguide Loss 1.32 db
 Waveguide Efficiency = 74%

Table 6. MK 25 waveguide measurement data.

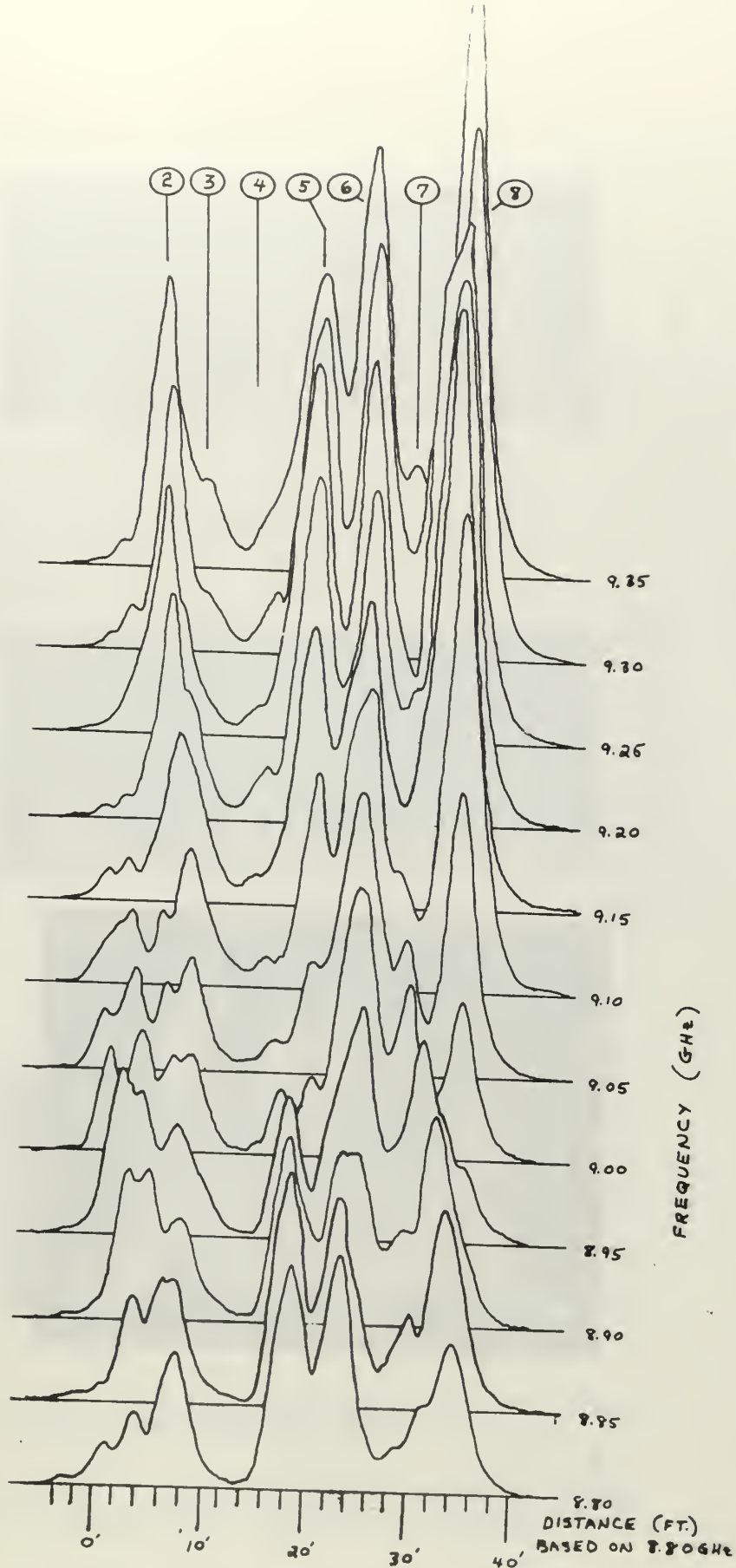


Figure 55. MK 25 radar waveguide reflections at frequencies 8.80-9.35 GHz.

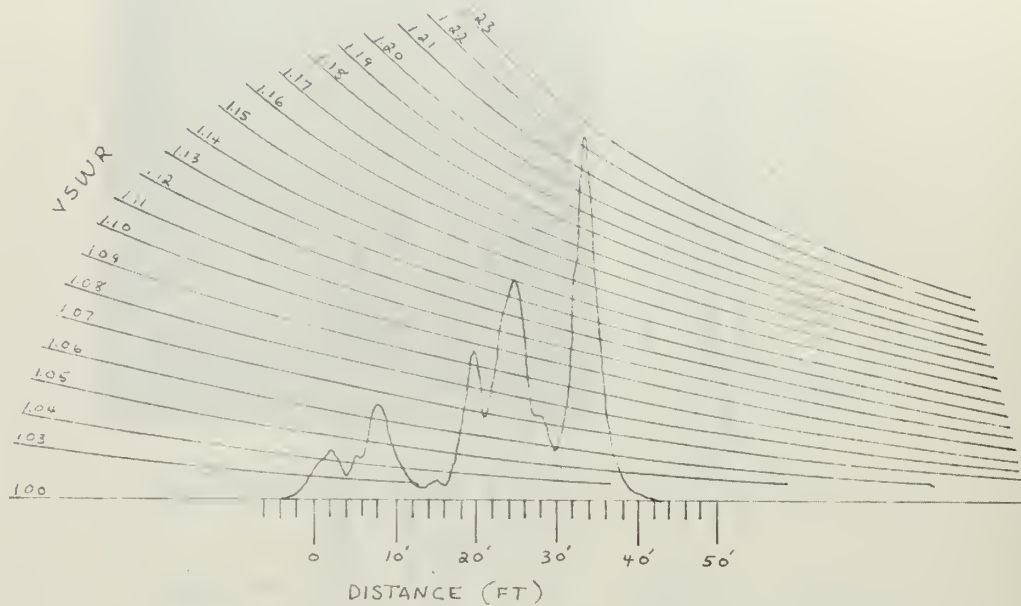


Figure 56. MK 25 radar waveguide reflections at 9.10 GHz.

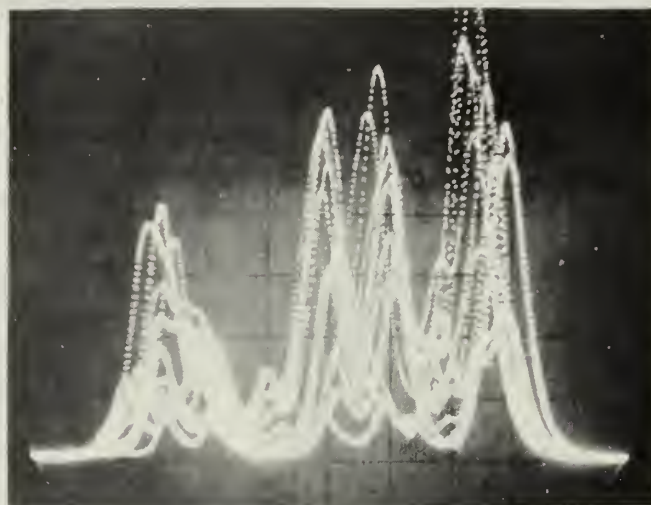


Figure 57. Multiple exposure of MK 25 radar waveguide reflections at frequencies from 8.8-9.35 GHz in 50 MHz steps.

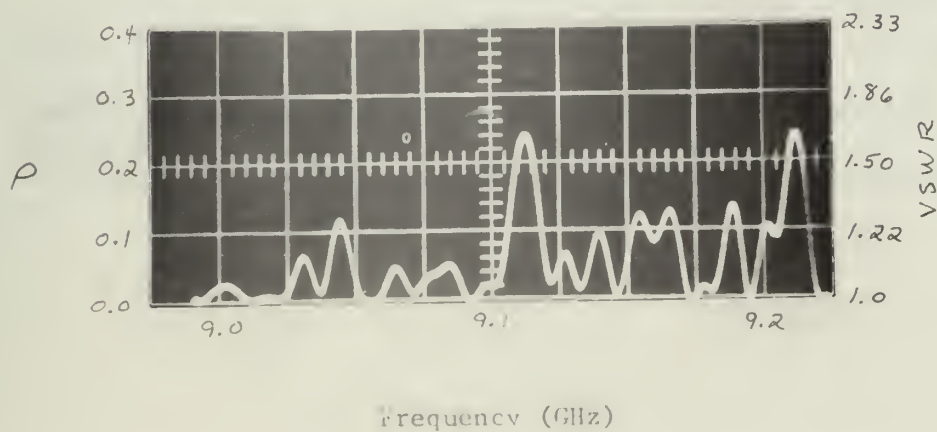
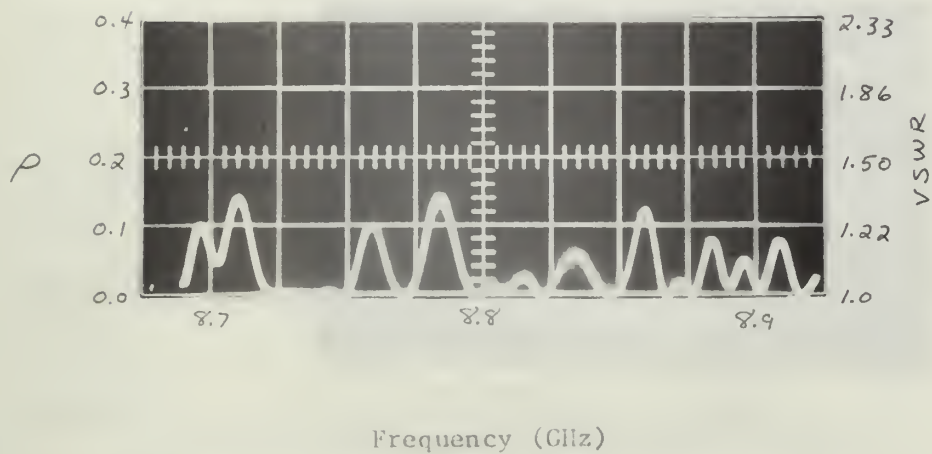
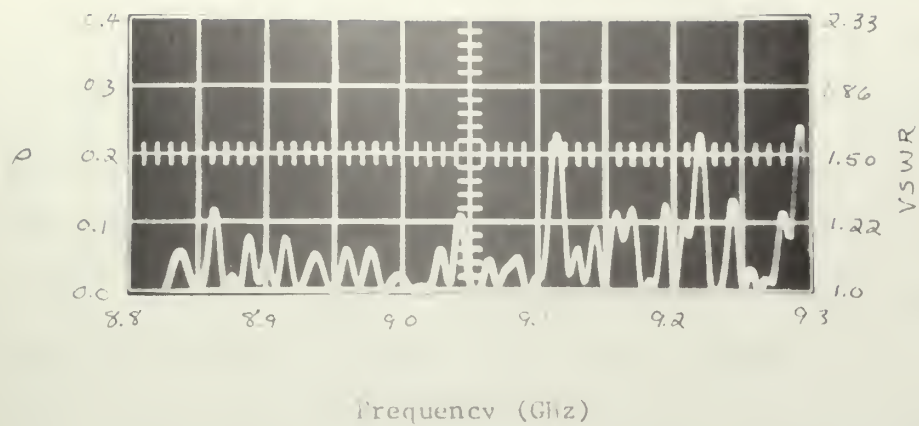


Figure 58. Voltage-reflection coefficient versus frequency, for 1.25 radar waveguide.



Scale: 40 ns/cm

Figure 59. L-band radar waveguide reflections

Several items are worthy of note concerning this L-band set-up. In this case a single traveling-wave tube was used as both modulator and amplifier for the c-w signal, providing better than 2 watts of peak power. All that was required to monitor the incident and reflected pulses was a dual-directional coupler, a 10-db pad and two standard, tunable, coaxial-detector mounts with IN-25 crystals. The same thyatron pulser was used to modulate the TWT grid. Even with no provision for precision measurement, the relative amplitude and position of discontinuities can be determined. Using only a display similar to that shown in Figure 59, any particular discontinuity can be located by probing the waveguide and noting the position of the probe reflection. Given a waveguide system with a defect, such a system could be used to isolate the particular discontinuity causing the problem, and to locate it on the waveguide.

These results confirmed the applicability of the proposed time-domain reflectometry techniques to the L-band frequency range and suggest that similar results could be achieved with other frequency-band radar waveguides.

CHAPTER V

CONCLUSIONS

The purpose of this research was the application of time-domain reflectometry to waveguide-system testing. The method which was developed--using nanosecond r-f pulses centered at the system's frequency of operation and having a bandwidth determined by distortion considerations or equipment limitations--proved far superior to existing time - or frequency - domain techniques for the location of faults in practical waveguide installations. It was demonstrated with this method that very useful waveguide testing could be carried out with commercially available laboratory equipment. Resolution of approximately 4 feet and sensitivity of better than 45-db return loss ($V_{SWR} \approx 1.01$) with an accuracy of plus or minus 2 percent was attained with a peak-pulse power on the order of 2 watts.

Existing time-domain reflectometers are not usable in waveguides because they employ waveforms having a frequency spectrum unsuited to waveguides. Furthermore, frequency-domain methods have been shown to be relatively unsatisfactory for locating faults in practical waveguide installations with multiple discontinuities.

A very simple trouble-shooting aid could be devised using an r-f pulse generator, together with either a circulator or dual-directional coupler, a detector and a sampling

oscilloscope. Using only this equipment, any faults can be located and identified from the position and relative magnitudes displayed on the oscilloscope. A particular discontinuity can then be pinpointed precisely by probing the waveguide while watching the oscilloscope display. Probing the waveguide by insertion of a reflecting piece into the nearest convenient flange is a means of positive fault location not requiring calibration of group velocity. If more accurate measurements are required, a shorting switch and a precision attenuator could be added in order to measure group velocity and waveguide attenuation. Precision measurement of discontinuities could then be carried out using the procedures outlined in Chapter IV. In either situation, a great advantage of such a system is that the immediate results of repairs can be viewed on the oscilloscope.

The ultimate realization of a pulse-generation method for use with waveguide TDR techniques will most likely be completely solid-state. The form taken could be that of a bulk-negative resistance device driven by a diode pulser. LSA diodes are currently on the market which can provide 2-nanosecond r-f pulses at power levels up to 100 watts.¹² Even more promising are Gunn diodes which could be used to produce 1 to 2-watt coherent r-f pulses, using a relatively low-power d-c supply. For use with either the LSA or Gunn diodes, a fast bias pulse could possibly be achieved using step-recovery diodes. These components could then be

assembled in a complete r-f pulse-generation package (including a power supply) which would be quite compact and convenient to use.

In any case, a relatively low-cost piece of test equipment could be achieved which would be very practical for waveguide-system evaluation or trouble-shooting, and which would require the very minimum of training to operate.

BIBLIOGRAPHY

1. Gould, K. E., United States Patent 2,345,932; March 1941.
2. Oliver, B. M., "Time Domain Reflectometry," Hewlett-Packard Journal, Vol.15, Feb. 1964.
3. Thompson, J. D. and Hart, A., "FDR: A New Deal For Faultfinders," Electronics, Aug. 19, 1968, pp. 96-99.
4. Schott, J. T., "The Lookator," Bell Laboratories Record, Vol.23, Oct. 1945, pp. 379-383.
5. Ross, G. F., "Series and Parallel Pulse-Forming Networks for the Generation of Microwave Energy," Microwave Journal, Sept. 1967, pp. 98-102
6. Beck, A. C., "Waveguide Investigations with Millimicrosecond pulses," Bell Systems Technical Journal, Jan. 1956, pp. 35-65.
7. Closson, H. T., Private Communication, S-F-D Laboratories, Apr. 19, 1968.
8. Burrus, C. A., "Millimicrosecond Pulses in the Millimeter Wave Region," The Review of Scientific Instruments, Vol. 28, Dec. 1957, pp. 1062-1065.
9. Pomeroy, A. F., "Improved Contact Flanges for Waveguides," Bell Laboratories Record, Oct. 1950, pp. 104-111.
10. Microwave Transmission Design Data, Ed. by Sperry Gyroscope Co., Inc., May 1944, p. 68.
11. Ginzton, E. L., Microwave Measurements, McGraw-Hill, (1957), pp. 142 and 268.
12. Karbowiak, A. E., Trunk Waveguide Communications, Chapman and Hall, Ltd., London, (1965), p. 34.
13. "LSA Diodes Go on Sale," Microwaves, Oct. 1967, pp. 76-78.

APPENDIX

Reflections from all fixed discontinuities are considered to be a single lumped discontinuity-- D. Reflections from the moveable parts are considered to originate from a single load-- L. The expressions for the voltage-standing-wave ratio due to D and L (considering the reflected voltages separately) are:

$$VSWR_L = \frac{E_I + E_L}{E_I - E_L} \quad \text{and} \quad VSWR_D = \frac{E_I + E_D}{E_I - E_D}$$

where E_I is the incident voltage. The ratio and product of these are:

$$VSWR_L VSWR_D = \frac{E_I + E_L + E_D + E_L E_D / E_I}{E_I - E_L - E_D - E_L E_D / E_I}$$

and

$$\frac{VSWR_L}{VSWR_D} = \frac{E_I + E_L - E_D - E_L E_D / E_I}{E_I + E_D - E_L - E_L E_D / E_I}$$

When the magnitudes of the reflected voltages are small compared to the incident voltage the following approximations can be used:

$$VSWR_{\max} = \frac{E_I + |E_D + E_L|}{E_I - |E_D + E_L|} \approx VSWR_L VSWR_D$$

$$VSWR_{\min} = \frac{E_I + |E_L - E_D|}{E_I - |E_L - E_D|} \approx \frac{VSWR_L}{VSWR_D}$$

This leads to the final form of the approximations:

$$VSWR_L \approx \sqrt{VSWR_{\max} VSWR_{\min}} \quad VSWR_D \approx \sqrt{\frac{VSWR_{\max}}{VSWR_{\min}}}$$

INITIAL DISTRIBUTION LIST

	No. Copies
1. Defense Documentation Center Cameron Station Alexandria, Virginia 22314	20
2. Library Naval Postgraduate School Monterey, California 93940	2
3. Commander, Naval Ship Systems Command Department of the Navy Washington, D.C. 20360	1
4. Commander, Naval Electronic Systems Command Department of the Navy Washington, D.C. 20360	1
5. Professor D. B. Hoisington Department of Electrical Engineering Naval Postgraduate School Monterey, California 93940	1
6. Professor G. L. Sackman Department of Electrical Engineering Naval Postgraduate School Monterey, California 93940	5
7. CDR S. C. Knock (Code 130) Quality and Reliability Assurance Officer San Francisco Bay Naval Shipyard, Mare Island Vallejo, California 94592	1
8. LCDR William B. Fletcher, Jr. USN Officer In Charge, Naval Shore Electronics Engineering Activity Great Lakes, Illinois 60088	1
9. Mr. J. C. King Radar Supervisor Department of Electrical Engineering Naval Postgraduate School Monterey, California 93940	1
10. Mr. Ross Seely Systems Supervisor Department of Electrical Engineering Naval Postgraduate School Monterey, California 93940	1

No. Copies

11. LT W. B. Shoemaker, Jr.
U.S. Naval Academy
Annapolis, Maryland 21402

1

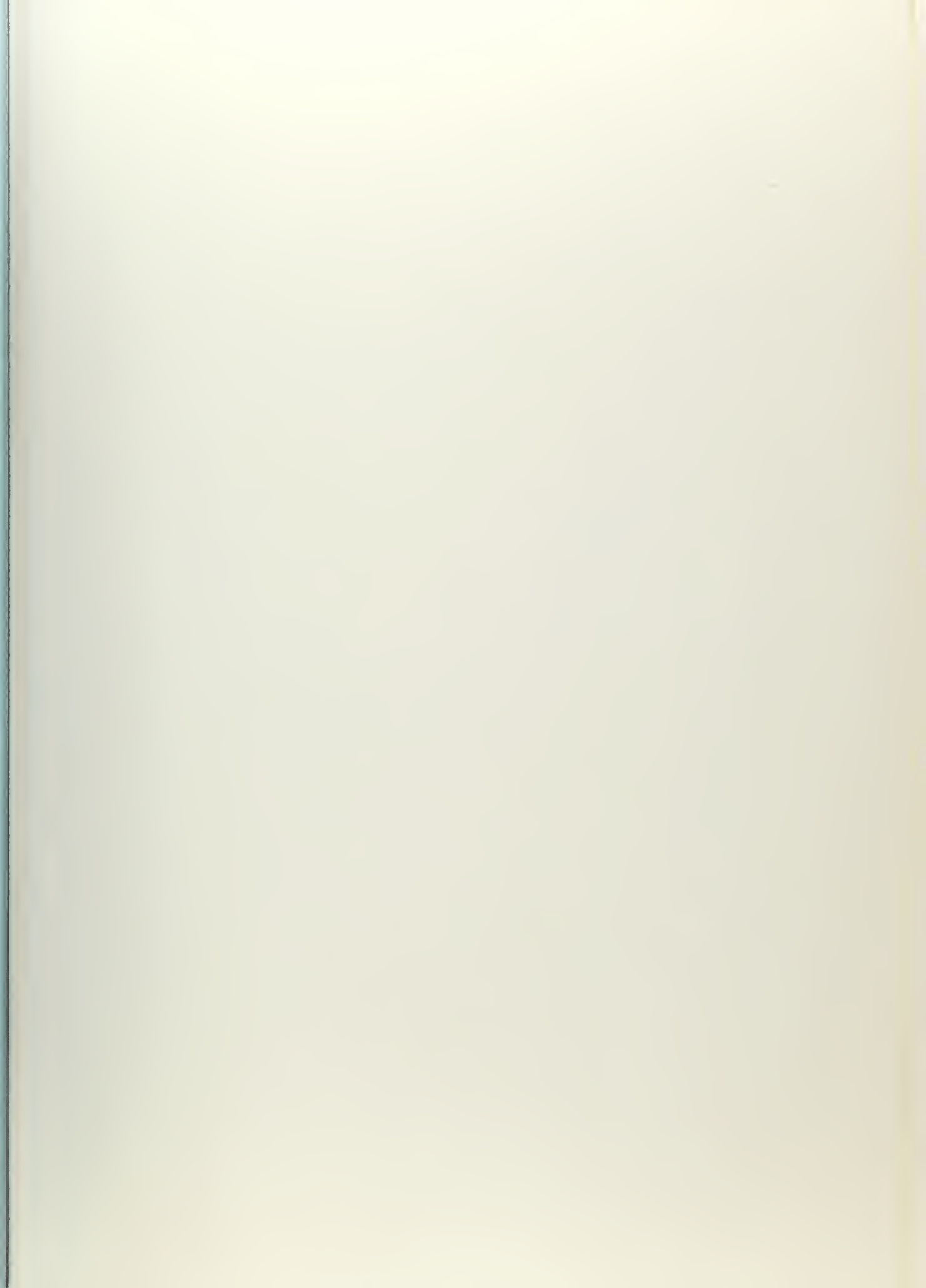
DOCUMENT CONTROL DATA - R & D

(Security classification of title, body of abstract and indexing annotation must be entered when the overall report is classified)

1. ORIGINATING ACTIVITY (Corporate author)		2a. REPORT SECURITY CLASSIFICATION	
Naval Postgraduate School Monterey, California 93940		Unclassified	
		2b. GROUP	
3. REPORT TITLE			
NANOSECOND R-F PULSES FOR WAVEGUIDE FAULT-FINDING			
4. DESCRIPTIVE NOTES (Type of report and inclusive dates)			
Thesis			
5. AUTHOR(S) (First name, middle initial, last name)			
William Bruce Shoemaker, Jr., Lieutenant, United States Navy			
6. REPORT DATE		7a. TOTAL NO. OF PAGES	7b. NO. OF REFS
September 1968		88	13
8a. CONTRACT OR GRANT NO.		9a. ORIGINATOR'S REPORT NUMBER(S)	
b. PROJECT NO.			
c.		9b. OTHER REPORT NO(S) (Any other numbers that may be assigned this report)	
d.			
10. DISTRIBUTION STATEMENT This document is subject to special export controls and its transmittal to foreign governments or foreign nationals may be made only with prior approval of the Superintendent, Naval Postgraduate School, Monterey, California 93940.			
11. SUPPLEMENTARY NOTES		12. SPONSORING MILITARY ACTIVITY	
		Naval Postgraduate School Monterey, California 93940	
13. ABSTRACT			
<p>A system has been developed for the location of waveguide discontinuities using nanosecond radio-frequency pulses with time-domain reflectometry techniques. The r-f pulse generation method used is discussed as well as the alternative methods investigated. Measurement-system design and procedures are outlined. Resolution on the order of 4 feet for reflections over 45-db return loss and accuracy of 2 per cent as compared to conventional methods are reported and various measurement examples are presented.</p> <p>Significant advantages of this system appear in locating imperfections in waveguides and other bandpass transmission systems, as compared to conventional c-w-standing-wave or trial-and-error methods.</p>			

14 KEY WORDS	LINK A		LINK B		LINK C	
	ROLE	WT	ROLE	WT	ROLE	WT
Waveguide fault-finding						
Nanosecond R-F pulses						
Time-domain reflectometry						
Microwave measurement						
Waveguide						







thesS4783

DUDLEY KNOX LIBRARY



3 2768 00415852 7

3 2768 000 99781 1

DUDLEY KNOX LIBRARY